ADDITIONAL CASE STUDY SIMULATIONS OF DRY WELL DRAINAGE IN THE TUCSON BASIN

PREPARED BY:

R. F. BANDEEN
WATER RESOURCES RESEARCH CENTER
UNIVERSITY OF ARIZONA

FINAL REPORT TO

PIMA COUNTY DEPARTMENT OF TRANSPORTATION AND FLOOD CONTROL DISTRICT

JUNE 1987

ADDITIONAL CASE STUDY SIMULATIONS OF DRY WELL DRAINAGE IN THE TUCSON BASIN

PREPARED BY:

R. F. BANDEEN
WATER RESOURCES RESEARCH CENTER
UNIVERSITY OF ARIZONA

FINAL REPORT TO

PIMA COUNTY DEPARTMENT OF TRANSPORTATION AND FLOOD CONTROL DISTRICT

JUNE 1987

ADDITIONAL CASE STUDY SIMULATIONS OF DRY WELL DRAINAGE IN THE TUCSON BASIN

TABLE OF CONTENTS

TABLE OF CONTENTS (continued)

TABLES

ILLUSTRATIONS

ACKNOWLEDGEMENTS

The patience of Dave Smutzer, Manager of the Long Range Planning Section, in the preparation of this report is gratefully acknowledged. Special thanks are extended to Dr. L. G. Wilson of the University of Arizona Water Resources Research Center, Principle Investigator of this Project, for his patience, technical guidance and assistance through the preparation of this report. Special thanks are also extended to Mr. Michael Osborn of the WRRC, Project Manager of this project, for his patience and assistance in the preparation of this report. Special thanks are extended to Dr. S. P. Neuman and Dr. J. Yeh, Professors of Hydrology at the University of Arizona, for their valuable technical consultation on the computer simulations. The assistance of graduate students Amado G. Guzman, Mariano Hernandez and Timothy P. Leo of the Department of Hydrology and Water Resources, University of Arizona, in performing the computer simulations, is gratefully acknowledged.

ADDITIONAL CASE STUDY SIMULATIONS OF DRY WELL DRAINAGE IN THE TUCSON BASIN

EXECUTIVE SUMMARY

Three case study simulations of dry well drainage were performed using the saturated-unsaturated groundwater flow model UNSAT 2. Each case simulated injection of storm water runoff water into a dry well from two five-year, one-hour storm events, separated by a 24-hour lag period. The first case assumed subsurface conditions of a uniform gravelly sand material from land surface to the water table at 100 feet below land surface. The second case assumed the same gravelly sand, underlain by a uniform sandy-clay loam material beginning at 30 feet below land surface and extending to the water table. The third case assumed the same conditions as in Case 2, except for a sandy loam soil replacing the sandy-clay loam material. Simulated subsurface flow of injection water for the first case was primarily vertical. The cross-sectional radius of the 95% saturated portion of the drainage plume reached a maximum of about nine feet during stormwater injection. In the second and third cases, horizontal flow took place at the layer boundary between the gravelly sand and underlying fine material. As a result, the cross-sectional radius of the 95% saturated portion of the drainage plume reached a maximum of about 27 feet for Case 2, and about 21.5 feet for Case 3. Arrival times of injection water at the water table varied from between 0.25 and 0.75 hours (Case 1), and between 130 and 150 hours (Case 2). Attenuation of water-borne pollutants in the vadose zone is related to the degree of exposure of drainage water to soil particle surfaces. The specific surface area of soil particles to which drainage water was exposed was used as an indicator of the relative degree of attenuation that may take place among the three cases. The ratio of specific surface area of soil matrix exposed to the portion of the subsurface reaching a state of 80% saturation was approximately 1 : 16.2 : 5.6 (Case 1 : Case 2 : Case 3).

INTRODUCTION

Concern over dry wells as a source of groundwater pollution in Arizona has led to state legislation requiring registration of existing and new dry wells and licensing of dry well drillers (Arizona House of Representatives, Bill 2229). Pima County and the City of Tucson have both recognized the need for hydrogeologic studies to be performed on dry wells to aid in the prediction of groundwater contamination associated with their use. In 1983 Pima County authorized funding for a field tracer study using an experimental dry well at the field station of the University of Arizona Water Resources Research Center (WRRC), Tucson, Arizona. Results were reported by Wilson (1983). Subsequently, Bandeen (1984) used the variably saturated flow model UNSAT 2 to simulate the subsurface flow system generated during operation of the dry well using a worst-case scenario which assumed that the well terminated above a completely impermeable geologic stratum. This study simulated the condition of maximum lateral movement of drainage water. The work described in this report focuses on the modeling of dry well drainage of storm water runoff for three additional subsurface conditions:

1. percolation of storm water from a dry well into a highly permeable zone above a water table;

2. percolation into a zone of highly permeable material underlain by a sandy clay loam material extending from a depth of 30 feet to the water table at 100 feet;

3. percolation into a zone of highly permeable material underlain by a sandy loam material extending from a depth of 30 feet to the water table at 100 feet.

These three case studies illustrate how dry well drainage water distributes itself through the course of a runoff event for uniform and layered subsurface conditions representative of the Tucson Basin. Results of the Wilson (1983) study suggested that subsurface attenuation of

pollutants may increase with lateral spreading of drainage water in the vadose zone. This lateral spreading increases for layered subsurface conditions in which vertical flow of drainage water is impeded by layers of low permeability. Where vertical flow is retarded at a transition to a layer of lower permeability, drainage water mounds up and spreads laterally along the layer transition. This phenomenon may increase vadose zone attenuation of pollutants by increasing both the degree and the duration of exposure of drainage water to vadose zone soil particles. The results of this study provide an illustrative example of how drainage plume distribution, rate of movement, and, indirectly, degree of attenuation, vary between uniform and layered soil conditions representative of the Tucson Basin.

STUDY OVERVIEW

Computer simulations of subsurface flow were performed for the three case studies assuming general hydrogeologic conditions observed at the WRRC field station. Previous studies by Dumeyer (1966) and Osborne (1969) indicate that a transition from a zone of relatively high sand and gravel content to a zone of relatively high silt and clay content exists in the vicinity of the WRRC experimental dry well at depth of approximately 30 feet below land surface. The constitution of the more permeable material above the layer transition at the site was determined from drill cuttings obtained during construction of the dry well. This highly permeable material is representative of sediments associated with high energy depositional environments, such as river channels, in the Tucson Basin. The Case 1 simulation addresses the situation of a dry well draining into a highly permeable material extending from land surface to the water table at a depth of 100 feet in order to illustrate rapid and direct infiltration of drainage water. This transition from a zone of relatively high permeability to a zone of relatively low permeability at a depth of 30 feet has been observed to cause the perching of drainage water introduced through the dry well and the subsequent lateral migration of this drainage water along the layer transition (Wilson, 1983). Inspection of City of Tucson well logs shows that abrupt transitions of geologic materials from zones of high hydraulic conductivity to zones of low hydraulic conductivity is a common occurrence in the Tucson Basin. As such, the associated phenomenon of perching and lateral migration of infiltration water, in areas where dry wells drain into such sediments, is also likely to be common. This hydrogeologic feature was included in the Case 2 and Case 3 simulations in order to model the phenomenon of perching and lateral migration of infiltration water. The constitution of the less permeable hydrogeologic material below the layer transition for Cases 2 and 3 is representative of subsurface conditions at the WRRC field site and of common Tucson Basin sediments. These simulations address the situation of a dry well draining into a highly permeable zone near the surface which is underlain by a hydrogeologic material of lesser permeability, inducing perching and lateral migration of the drainage water.

HYDROGEOLOGIC SETTING

Drainage and tracer tests were conducted on an experimental artificial recharge well at the field laboratory of the WRRC. Dumeyer (1966) characterized the vadose zone sediments at the WRRC field site as a series of alternating beds of varying sand, silt, clay and gravel composition. Dumeyer described the vadose zone deposits as consisting of three major units: Quaternary alluvium on the surface, underlain by Quaternary Basin Fill, which is in turn underlain by Tertiary sediments. Sieve analysis performed by Osborne (1969) and neutron logs taken from two-inch diameter access holes near the dry well indicate that the transition between the Quaternary Basin Fill and Quaternary alluvium occurs on the average at a depth of about 30 feet in the vicinity of the field site. Drilling time logs for access holes in the vicinity of the dry well show peak values in the zone of 20 to 30 feet below land surface. Longer drilling time generally corresponds to coarse subsurface materials such as sands, gravels, and cobbles. The drilling logs also show loss of drilling fluid at these depths, which is indicative of a zone of highly permeable material. Grain size distribution analyses performed by Osborne exhibit the following trends: 1) generally high sand and gravel content from land surface to 30 feet, with maximum gravel content from 20 to 30 feet; and 2) increased silt and clay content beginning at approximately 25 to 30 feet. Neutron logs obtained from the access holes during recharge experiments illustrate an accumulation of water in the zone of 25 to 35 feet and subsequent lateral movement of the accumulating water (Wilson, 1983). All of these observations support the conclusion of a stratigraphic transition from a highly permeable sand and gravel unit to a less permeable loam material at approximately 30 feet below land surface. This observed field condition serves as the basis for the layered subsurface conditions assumed in the Case 2 and Case 3 simulations.

The depth to water at the WRRC field site is approximately 110 feet. A depth of 100 feet was assumed in the simulations to help optimize the size

of the model grid. A depth of approximately 100 feet to groundwater is representative of many parts of the Tucson Basin.

UNSATURATED FLOW AND MODELING OF DRY WELL INJECTION

STORMWATER INJECTION INTO THE VADOSE ZONE

Dry wells are usually designed to inject runoff water into highly permeable soil materials. The sediments that extend from land surface to the water table constitute the "vadose zone." Prior to storm water injection, the vadose zone surrounding a dry well is in a state of residual saturation. The interstices between the soil grains are partly filled with water remaining from previous recharge events. The remaining pore space is filled with air. Sediments in this state are described as "unsaturated." The water in the interstices of unsaturated soil is subjected to capillary forces that create a negative pressure or suction within the soil matrix. When storm water is introduced via a dry well, the air in the soil interstices is expelled and the sediments around the dry well become saturated. As the water injected via the dry well is under the pressure caused by the weight of water in the dry well shaft, a hydraulic gradient is generated which causes the water to move into the surrounding unsaturated sediments. This flow takes place in both the lateral and vertical directions under the combined effects of the pressure differential and gravity. In uniform soils, gravity eventually becomes the dominant driving force and the vertical flow component becomes more pronounced than the horizontal. In layered soils the downward movement of water may be impeded by beds of relatively low permeability and the water may spread laterally over considerable distances before resuming downward movement.

As storm water injection continues during and after a precipitation event, the saturated region below and surrounding the dry well continues to expand. If the volume of runoff water is sufficient, this saturated region may eventually extend to the water table. If the volume of runoff water is relatively small, the front of saturation may remain and possibly stabilize above the water table.

PRINCIPLES OF FLOW IN THE VADOSE ZONE

The rate at which water can be injected into the vadose zone from a dry well, as well as the manner and rate at which the injected water propagates through the vadose zone to the aquifer, are determined by the level of water in the dry well shaft, the initial water content of the surrounding and underlying soils, and the hydraulic properties of these soils. The rate of flow through both the saturated and unsaturated regions is controlled by an equation for flow in porous media known as Darcy's Law. According to Darcy's Law, the volume of water crossing a unit area of soil in a unit of time, known as "specific flux," is directly proportional to the rate at which hydraulic head decreases in the direction of flow per unit distance, know as "hydraulic gradient." The constant of proportionality, usually designated by the letter K, is known as "hydraulic conductivity," and has the same dimensions as velocity. Values of hydraulic conductivity are typically measured in units of centimeters per second, feet per day and other related units. Values of hydraulic conductivity for various soil types vary by several orders of magnitude. Values for hydraulic conductivity for a clean sand and gravel typically range from 100 feet per day to 1,000 feet per day. Values for fine sand typically range from 1 foot per day to 100 feet per day. Values for silt and mixtures of sand, silt and clay typically vary from 0.001 feet per day to 1 foot per day. Dense clays generally have hydraulic conductivity of less than 0.001 feet per day (U.S. Dept. of the Interior, 1977).

Unsaturated Hydraulic Conductivity

Hydraulic conductivity, except for very minor changes resulting from variations in temperature and fluid density, is a constant property of the soil and the fluid that penetrates it. In the saturated zone below the water table, water maintains a relatively uniform temperature so that K depends solely on the permeability of the soil. In the vadose zone, the soil pores are filled with both water and air, and K depends on the relative

amounts of these two fluids. The higher the water content, expressed as volume of water per bulk volume of soil, the larger the value of unsaturated K. Each soil has a functional relationship between unsaturated K and water content. Just as K varies with water content, so does specific flux. The process of injection and flow propagation from a dry well depends on the degree of saturation of the soil material. "Relative" hydraulic conductivity is the ratio between the hydraulic conductivities of a soil under unsaturated and saturated conditions. A graph of relative hydraulic conductivity versus water content is shown in **Figure 1.**

When permeability varies from location to location in a given layer of soil, the soil material is said to be "heterogeneous." When permeability varies depending on direction at a given location, the soil material is said to be "anisotropic." Conversely, when soil permeability is constant with respect to location and direction in a given layer of soil, that soil material is described as "homogeneous" and "isotropic." The use of layered subsurface conditions in the Case 2 and Case 3 simulations introduces heterogeneity and anisotropy between layers. Within the layers themselves, however, homogeneity and isotropy are assumed.

Soil Moisture Retention

For a soil in a variably saturated state, i.e. undergoing wetting or drying, there exists a unique relationship between water content and soil pore pressure. This functional relationship, the graph of which is called the soil moisture "retention curve," is another property characteristic of a given soil which controls unsaturated flow in the vadose zone. Generally, as the water content increases, the negative, or capillary, pressure becomes less negative. Negative pressure head is also known as "suction head," which is plotted as a positive quantity, as in the soil moisture retention curve shown in **Figure 2.** Soil retention curves are generally determined either in the laboratory using a pressure chamber, or in the field using instrumentation sensitive to soil pore pressure and moisture content.

Specific Moisture Capacity

By taking the reciprocal of the slope of the soil moisture retention curve, a third characteristic unsaturated flow property, the "specific moisture capacity" of the soil as a function of water content, is obtained. Specific moisture capacity may be viewed as the volume of water the soil absorbs per unit decrease in suction. An example of a specific moisture capacity curve is shown in **Figure 3**. The specific moisture capacity as a function of water content is used in calculating mass balance in flow through unsaturated soil. Mass balance and Darcy's Law are the two physical principles that underlie most models of groundwater flow through the subsurface under both saturated and unsaturated conditions. The same principles form the basis for the variably saturated flow model UNSAT 2 used in these simulations.

Infiltration

Infiltration is the process by which water from a surficial source advances underground. It is important to note that infiltrating water does not penetrate the subsurface in a "plug flow" process where the infiltration front is marked by an abrupt transition from completely dry to completely saturated soil. Instead, infiltration is characterized by a condition of soil saturation just below the water source, which tapers off gradually to some volumetric water content close to the saturated water content, θ, at some depth, y, below the surface (Figure 4). Below point y, moisture content tapers off gradually to the value of "background," or residual moisture content, θ_n, prevailing in the soil. This zone, where moisture content decreases from close to saturation to residual moisture content, is known as the "capillary fringe" of the drainage plume. This advancing capillary fringe of the drainage plume marks the "infiltration front," which steadily progresses with time, as shown in Figure 4. Between land surface and point y, moisture content is at a high degree of saturation but still below 100% saturation. In the contour plots of saturation illustrating the

results of the model simulation, point y is approximated by the level of 95% saturation, and marks the point of advance of the infiltration front in the soil below and surrounding the dry well.

PROGRAM UNSAT 2

The UNSAT 2 model was developed by Dr. Shlomo P. Neuman, presently Professor of Hydrology at the University of Arizona, and was originally documented in Neuman et al. (1974). The mathematical basis of the model was described in a series of papers by Neuman (1975) and Neuman et al. (1975). A variety of applications have been reported by Feddes et al. (1974), Kroszynski and Dagan (1975), Wei and Shieh (1979), Zaslavsky and Sinai (1981) and others. For a thorough discussion of the background theory and mechanics of the model, the reader is referred to the model Documentation and User's Guide (Davis and Neuman, 1983). The program can be used for the analysis and computer simulation of groundwater flow in partially saturated and saturated porous media. UNSAT 2 can treat flow regions delineated by irregular boundaries and composed of layered soils. The program requires as input a delineation of the flow region geometry; the initial distribution of water content throughout the flow region; the moisture retention, relative hydraulic conductivity and specific moisture capacity as functions of water content for each soil type contained within the flow region; and the physical and mathematical conditions that prevail along the boundaries of the flow domain. Typical boundary conditions include "no flow," which designates an impermeable boundary, and known hydraulic or pressure head, such as would exist in a dry well with a sustained height of water in the shaft due to storm water runoff drainage. The program then solves a partial differential equation derived by Richards (1931) which embodies the physical principles of mass balance and Darcy's Law.

For these simulations, axisymmetric flow conditions were assumed. In other words, the soil is assumed to be uniform in every direction emanating radially outward from the center of the dry well. To solve the Richards

equation over the flow region, consisting of the soil surrounding and below the dry well to the water table in the case of this simulation, UNSAT 2 uses a computational scheme known as the Galerkin finite element method. This finite element method requires that a radial cross section representing the flow region be subdivided into a number of triangular or quadrilateral subregions called elements. The result is a mesh of elements denoted as a finite element grid (**Figure 5**). The corners of these triangles and quadrilaterals are called nodes. The grid represents an area measuring 100 feet horizontally from the center of the dry well, and 110 feet in the vertical direction. The term "axisymmetric" implies that the actual flow region simulated is derived by rotating the entire grid 360 degrees about its left-most border. Using an algebraic approximation to the Richards equation, the program computes hydraulic heads, pressure heads and water contents at all the nodes of the finite element grid at progressive points in time. In these simulations, the initial time is at the onset of injection into a dry well accompanying a storm event. The solution progresses forward in time through the first storm event, then through a 24-hour drainage period, followed by a second storm and subsequent drainage period. UNSAT 2 also computes the rate of water flow at each boundary node. From these data one can monitor the total rate of injection for the dry well.

Computational Considerations

To solve the Richards equation by the finite element method, the unsaturated soil properties in each element must be known at the beginning and end of each time increment. In reality, these properties are known only at the beginning of the time increment. As time progresses, the pressure at each node changes and this in turn causes a change in the soil parameters of hydraulic conductivity, water content and specific moisture capacity. These changes cannot be predicted without knowing the pressures at all the nodes at the end of the time increment, yet the pressures cannot be computed without knowing how the soil parameters will change with time.

Mathematically, this amounts to having as many unknowns as there are variables in the equation. To solve for the unknowns in this type of equation, at the end of each time increment, the soil parameters are updated to reflect the most recent pressure calculations at all the nodes, and the solution for the time increment is repeated with these updated values. This process is repeated for each time increment until the previous and updated pressure values differ by not more than a user-specified tolerance. The iterative process therefore provides an approximate solution. A smaller tolerance implies a more accurate solution, but also implies more computing time and its associated expense.

As the solution progresses through time, the pressure distribution in the flow region and its associated moisture content distribution are saved on separate files for use in creating contour plots. These contour plots give a graphic representation of the distribution of flow from a dry well at various stages of storm water recharge events and intermittent drainage.

UNSAT 2 was originally developed for use on an IBM mainframe computer and was later adapted to CDC and Cyber computers. The program is written in the ANSI standard Fortran 77 language and is therefore easy to modify for use on other computers. For these simulations, the Cyber 175 computer at the University of Arizona was employed.

DERIVATION OF MODEL INPUT PARAMETERS

Three different soil materials were used in these simulations. The first material constitutes the entire flow region in the Case 1 simulation, and the zone from land surface to a depth of about 30 feet in the Case 2 and Case 3 simulations. This material comprises primarily gravelly sand and sandy gravel, and is called Material 1 for the purposes of this study. Material 1 is patterned after soil removed from borehole cuttings during construction of the dry well at the WRRC field site, and is representative of the soil zone into which the dry well injects water. The second

material, Material 2, is patterned after a clay/silt loam type soil documented in a previous soil study of Tucson Basin soils performed by a University of Arizona graduate student (Coelho, 1974). The third material, Material 3, is patterned after a sandy loam type soil documented in a separate earlier study of Tucson Basin soils by another University of Arizona graduate student (Guma'a, 1978). All three of these materials are common in the Tucson Basin and are representative of soils of high (Material 1), low (Material 2), and moderate (Material 3) permeability.

Relative Hydraulic Conductivity Curves

Field and laboratory measurement of relative hydraulic conductivity, as a function of water content, is a very time-consuming and expensive process. A computer model developed by van Genuchten (1978) allows for the derivation of the relative hydraulic conductivity, as a function of water content curve, from the soil moisture retention curve. The model employs a closed-form analytical method to relate the shape of the moisture retention curve to the inferred shape of the relative hydraulic conductivity curve. This model was employed for all three of the soil materials used in the simulation to produce the relative hydraulic conductivity curves shown in **Figures 1, 6, and 9.**

Moisture Retention Curves

The moisture retention curve, which specifies the relationship of negative pressure head, or suction head, to water content in the soil, was obtained using laboratory methods for Material 1, and using in situ and laboratory methods for Materials 2 and 3 (Coelho, 1974, and Guma'a, 1978). A special adjustment which accounts for the presence of gravel and cobbles was made to the Material 1 curve using the method of Bouwer (1984). A spline function curve-fitting program was used to smooth and fit the curves

to laboratory and field data. The moisture retention curves for Materials 1 through 3 are shown in **Figures 2, 7, and 10.**

The moisture retention curves for a given soil vary in accordance with whether the soil is being wetted or is draining. This phenomena is known as hysteresis. Generally, for a given suction head, water content in the soil will be greater during drying than during wetting. The moisture retention curves used in this study represent the main drying soil moisture retention curve for each of the three soil materials. Insofar as the computer model used in the simulations does not address the phenomenon of hysteresis, its effects were not considered in this study.

As a result, some discrepancy between the moisture content predicted by the model, and that actually occurring for a given soil material in the field, is likely to occur during the wetting (storm water recharge) phase of the simulations. In using a drying moisture retention curve to simulate a wetting condition, soil water content for a given suction head will be slightly overestimated during the wetting phase of the simulation. As such, relative hydraulic conductivity will also be slightly overestimated (for the wetting phase), resulting in a higher rate of movement of recharged water during the wetting phase. Consequently, the predicted rates of vertical and horizontal movement of recharge water during a recharge event will err slightly to the high side.

Additional laboratory work, to define the main wetting loop of the soil moisture retention curve using an improved model for each material, and additional model simulations would have to be conducted to incorporate the hysteretic effects of the soil.

Specific Moisture Capacity Curves

The relationship of specific moisture capacity to water content for the three soils was obtained using a computational routine in the UNSAT 2

program which calculates the inverse of the slope of the moisture retention curve at various values of water content. The spline algorithm routine was employed to smooth the curves. The specific moisture capacity curves are shown in **Figures 3, 8, and 11.**

Saturated Hydraulic Conductivity

UNSAT 2 was used to simulate conditions observed in the dry well tracer tests performed by Wilson (1983) to calibrate a value for saturated hydraulic conductivity, known as K_S. This was accomplished by using known dry well inflow rates from the field tests and measurements of the height of water in the dry well shaft. The field-measured height of water in the dry well shaft for a given recharge test was specified as a boundary condition in the model. The assumed value for K_S was then varied through a series of experimental computer runs until the inflow rate into the dry well, as computed by the model, matched the inflow rate observed in the field. The resulting calibrated K_S for Material 1 was 6.7 feet per hour, or about 161 feet per day. The K_S values for Materials 2 and 3 were calculated using field and laboratory methods. The values of K_S for Materials 2 and 3, as reported by Coelho and Guma'a, were 0.29 feet per hour and 1.0 feet per hour, respectively.

CASE STUDY SIMULATIONS

STORM WATER RUNOFF INPUT TO A DRY WELL

Runoff for a five-year, one-hour storm, calculated specifically for the Tucson Basin from a Soil Conservation Service standard hydrograph, was used as input for the dry well in all three simulations. The influx of storm water from this precipitation event was input to the model twice, separated by a 24-hour lag period. This simulates the effect of multiple storms, such as those that may occur almost daily in the Tucson area during the monsoon season. The volume of runoff from this storm was calculated as approximately 5,000 cubic feet. The manufacturer of the experimental dry well at the WRRC field station indicated that over the long term, most dry wells are designed to accommodate a flow of approximately 0.5 cubic feet per second (cfs). Though this intake rate varies with the size, age and quality of runoff water for specific dry wells, the rate of 0.5 cfs was specified by the manufacturer as the expected long-term intake rate for a Maxwell Type III dry well servicing one paved acre (De Tommasso, 1984). With this in mind, the rate of dry well recharge was controlled during each simulation to average about 0.5 cfs for the duration of each of the storm recharge events. Using this criterion, the 5,000 cubic feet of run-off for each of the 5-year, 1-hour storms was recharged for about 10,000 seconds, or 2.77 hours.

CASE 1 SIMULATION

The first case study was a hypothetical simulation that assumed a flow region made up entirely of Material 1 soil. Actual field data show that soil similar to Material 1 in texture and hydraulic properties exists only to a depth of about 30 feet. However, in areas of the Tucson Basin where river channel deposits prevail, it is common for these materials to exist in depth intervals of 100 feet or more. The Case 1 simulation was designed to address the situation where the entire vadose zone is composed of a highly

permeable material. This simulation of dry well drainage was expected to show, relative to the other two, a maximum rate of vertical infiltration, a minimum time of arrival of drainage water at the water table, and a minimum cross-sectional area of the drainage plume, allowing for a minimal amount of attenuation of contaminants potentially contained in the runoff water. Attenuation of water-borne contaminants in the vadose zone constitutes a "filtration" of water by the soil, and includes such processes as adsorption, ion-exchange, complexation and precipitation. By limiting the surface area of soil particles to which the water is exposed, and the time of that exposure due to rapid infiltration, these processes will be at a minimum in the Case 1 simulation. Essentially, the Case 1 simulation depicts the worst case of the three with regard to the likelihood of groundwater contamination via the dry well.

CASE 2 SIMULATION

The second case study incorporates the concept of a layered flow region, as observed at the WRRC field station site. In this case, the zone extending from land surface to a depth of 30 feet consists of Material 1, and the remainder of the flow region from 30 feet below land surface to the water table consists of Material 2. Lithologic data at the field site indicate that the zone below 30 feet is actually composed of loam material with varying degrees of sand, silt and clay. The Case 2 simulation assumes the uniform existence of the Material 2 sandy clay loam below 30 feet. The existence of a soil material transition from a material of relatively high permeability (Material 1) to a material of relatively low permeability (Material 2) at 30 feet causes a retardation of downward movement of drainage water and, as more water builds up at this transition, lateral flow along the material transition. This case study provides a contrast to the Case 1 study in that the plume of drainage water emanating from the dry well is forced to percolate through a material of much lower permeability and therefore moves much more slowly. Furthermore, by spreading out laterally along the material transition, the plume of drainage water is distributed

over a much larger area, exposing it to a much larger proportion of soil material. As a result, water-borne constituents in the dry well influent undergo a much greater proportion of the attenuation processes associated with the soil material. The greater cross-sectional area of the plume of drainage water implies a greater opportunity for dilution of drainage water with the groundwater when the drainage water percolates to the water table. In this case, relative to the other two, rate of downward infiltration will be at a minimum, time of arrival of drainage water at the water table will be at a maximum, and the degree of available soil surface area for attenuation will be at a maximum. The Case 2 simulation depicts the scenario where dry well-associated groundwater contamination is least likely to occur.

CASE 3 SIMULATION

The third case study was designed to present an intermediate case in comparison to the other two. As in Case 2, a layered condition is assumed, but the soil material below a depth of 30 feet to the water table comprises Material 3, a sandy loam. Also, as in Case 2, the soil extending from land surface to a depth of 30 feet comprises Material 1. The results were expected to be similar to those of Case 2, except that the degree of lateral spreading at the material transition is not as great, and the rate of infiltration to the water table is somewhat greater. The Case 3 simulation is necessary to provide a moderate contrast to the other two, more extreme cases; it is also representative of soil conditions at the WRRC field site and in the Tucson Basin in general.

INTERPRETATION OF RESULTS

At specified times throughout the simulations, information concerning the location and pressure head of all points in the grid was recorded for use in a contour mapping routine at a later time. At each specified point in time, contour maps of the degree of saturation and hydraulic head

distributions throughout the flow field were plotted. The "degree of saturation" of a portion of soil is simply the ratio of its given volumetric water content to its volumetric water content at saturation. Contours of the degree of saturation for the soil surrounding the dry well provide a visual representation of the distribution of subsurface water introduced via the dry well. The "hydraulic head" is a measure of the total potential and kinetic energy of a particle of fluid at a given point in time. For infiltration of water in soils, where fluid velocities are relatively small, the majority of this energy is potential. The hydraulic head consists of the sum of the pressure head and the elevation of a given fluid particle above a pre-determined datum. The distribution of hydraulic head in the flow region determines the flow paths of the drainage water. Each of the contour plots represents a two-dimensional distribution of saturation or hydraulic head throughout the finite element grid, which represents an axisymmetric slice of the area surrounding the dry well. The true representation of saturation or hydraulic head is obtained by rotating the plot 360 degrees about its left-most axis, representing the center of the dry well. The horizontal dimensions of the contour plots vary from 50 to 100 feet.

Specific Soil Surface

The size of the saturated portion of the drainage plume is an indication of the total surface area of soil particles to which the drainage water is exposed. The geochemical processes that cause soil to act as a "filter" for some water-borne contaminants such as ion exchange and adsorption, are directly related to the degree of exposure of water to soil particle surfaces (Hillel, 1971). As the radius of the drainage plume increases, so does the degree of exposure of the water to soil particles and their associated attenuation and filtration mechanisms.

For comparing the relative degree of exposure of drainage water to vadose zone soil particles, the maximum soil surface area contained within

the region of 80% saturation was estimated for each of the three cases. These estimates provide a measure of the relative degree of attenuation that may be expected to take place between the three cases. First the total bulk volume of soil within the zone of 80% saturation is calculated, assuming an approximate geometric shape of the drainage plume (i.e. some combination of circular cylinders, cones and spheroids).

DISCUSSION OF RESULTS

CASE 1 SIMULATION

Storm 1

From the beginning of injection to a time of 0.25 hours, the zone of 95% saturation had moved from the bottom of the dry well at a depth of 23.5 feet to a depth of about 36 feet below land surface (**Figure 12a**). The rate of infiltration was initially high due to the dry condition of the soil, which caused a large pressure head gradient between the dry well injection water, under a positive pressure, and the surrounding soil, under a negative pressure. As time progressed, the soil zone below a depth of 36 feet remained "unsaturated," but reached ever higher degrees of saturation. The downward progress of infiltration water is illustrated by the s = 0.95 contour, where soil is very close to saturation. From 0.5 hours to 1.0 hours, the average downward velocity of the soil zone equal to or greater than 95% saturation was about 21.75 feet per hour. From 1.0 to 1.5 hours, this velocity decreased to an average of about 17 feet per hour. Generally, the average vertical velocity of infiltrating water will continue to decrease until rate of advance reaches a stable deep percolation rate. The deep percolation rate is calculated as the hydraulic conductivity divided by the water-filled porosity of the soil (Kirkham and Powers, 1984). In this case, the zone of 95% saturation reached the water table at 100 feet below land surface between 1.5 and 2.0 hours after the beginning of injection (**Figure 13a**).

The water table is defined as the line of zero pressure head at a depth of 100 feet, marking the saturated surface of the regional aquifer. From a time of 2.0 hours to 2.722 hours, the contours of degree of saturation remained approximately the same. At a time of 2.722 hours of infiltration

at the design flow rate of 0.5 cfs, the entire volume of runoff from the first storm event had been injected through the dry well.

The total hydraulic head distribution for the flow region at the end of injection of storm water from the first storm is shown in Figure 17a. The dashed lines represent the approximate flow path of the injected water moving out from the dry well into the vadose zone. These flow paths consistently follow lines perpendicular to line of equal head. Due to a pressure gradient induced by the weight of the column of water in the dry well, some horizontal flow of water takes place near the dry well. Below a depth of about 30 feet, the flow direction is predominantly vertical. As mounding occurs at the water table directly beneath the dry well, the weight of mounding water induces a pressure gradient in the saturated zone below the water table, again inducing horizontal flow.

PLUME DISTRIBUTION: Throughout the period of injection of storm water from the first storm, the radius of the saturated portion of the drainage plume emanating from the center of the dry well reached a maximum of about 7.75 feet from the center of the dry well. This maximum occurred at a depth of about 30 feet below land surface. As the drainage plume approached the water table, this radius became smaller. The radius of the 95% saturated portion of the drainage plume was at a minimum of about 5.5 feet above the water table. This narrowing of the cross-sectional area of the drainage plume with depth was a function of the relatively high velocity of vertical movement of drainage water.

Taking the 80% saturated portion of the drainage plume to be approximately the shape of a right circular cylinder of average radius 10.5 feet and height 83.5 feet (the distance from the top of the column of water in the dry well to the water table), the total volume of soil bulk contained within the region of 80% saturation was approximately 29,000 cubic feet. Following the method of White (1979), this corresponds to a total soil surface area of about 2.777514 x 10 square meters for soil Material 1.

24-Hour Drainage Period

Following the termination of inflow of storm water after 2.72 hours, water injected into the soil via the dry well during the first storm drained downward toward the water table. Flow during this phase of the simulation was entirely unsaturated by a time of 2.0 hours after cessation of injection from the first storm (**Figure 13c**). The position of the saturation = 0.80 contour illustrates this downward movement of residual drainage water over time. From a time of 2.0 to 9.0 hours of post-storm 1 drainage, the s = 0.80 contour moves from a level of about 70 feet above the water table to about 29 feet above the water table. By the time of 15 hours of drainage, the soil moisture in the zone of 80% saturation has drained to about 10 feet above the water table (**Figure 14c**). From 15.0 to 24.0 hours of post-storm 1 drainage, the saturation distribution in the flow region changes very little (**Figures 14c and 15a**). As the residual moisture in the soil at this point is under a higher soil suction, movement through the soil takes place much more slowly.

Storm 2

The 24-hour drainage period was immediately followed by injection of storm water from a second five-year, one-hour storm. The saturation plot for the time of 15 minutes of injection of water from the second storm indicates that the zone of 95% saturation advanced to a level of about 51 feet below land surface, about 15 feet further than for the same period during storm 1 (**Figure 15b**). This resulted in a higher downward flow velocity than that of the first 15 minutes of injection for the first storm. This higher rate of deep percolation is due to the higher level of moisture in the soil. The background soil water content in the soil during injection of the first storm runoff was about 13%, corresponding to a level of saturation of 43%. The background moisture of the soil at the beginning of injection of runoff from the second storm ranged from about 18% to 23%, corresponding to a level of saturation of about 60% to 75%. The higher

background water content was due to moisture retained in the soil from infiltration of runoff water from the first storm. The higher background moisture content gave rise to a higher hydraulic conductivity for the soil below the dry well. By a time of 0.75 hours of injection of storm water from the second storm, the flow region had a saturation distribution similar to that at a time of about 2.0 hours during the first storm. From a time of 0.75 hours to 2.66 hours of storm water injection, the distribution of saturation remained essentially the same (**Figures 15c and 16a**). The total time of injection of runoff from the second storm was less than that for the first storm, again because of the higher initial rates of infiltration.

The distribution of hydraulic head in the flow region at the end of injection of water from the second storm is similar to that at the end of the first storm (**Figure 17b**). Note that higher values of hydraulic head existed in the saturated zone below the water table at the end of injection from the second storm. At that point, 10,000 cubic feet of water had been injected, and additional mounding at the water table had caused a greater pressure buildup due to the added weight of the mounded drainage water. This added pressure again induced horizontal flow below the water table, as shown by the flow lines in **Figure 17b**.

Post-Storm 2 Drainage

During the period of drainage following the second storm, flow in the system was predominantly unsaturated flow. At a time of 0.5 hours following the influx of the 5,000 cubic feet of runoff from the second storm, the zone of 95% saturation had already dissipated into the regional ground water system (**Figure 16b**). The majority of the flow region at that time was in a state of between 75% and 95% saturation. Though no saturated areas remained in the vadose zone, a considerable amount of moisture remained bound in the soil pores. Throughout the first six hours of drainage, the portion of the flow region characterized by water under a saturation of 80% moved downward at a rate of approximately five to six feet per hour. At a time of 12 hours

of post-storm 2 drainage, this portion of the flow region had advanced to approximately 10 feet above the water table (**Figure 18a**). At a time of 24 hours of post-storm 2 drainage, this portion of the flow region was completely assimilated by the regional ground water system. Typically, given sufficient time, the soil will reach a characteristic minimum moisture content, having undergone the maximum possible degree of drainage by gravity. This minimum level of soil moisture is known as "field capacity."

CASE 2 SIMULATION

The main difference in the Case 2 simulation was the existence of a second, less permeable soil material beginning at a depth of 30 feet below land surface. It was expected that, to some degree, this layer would cause an obstruction to downward flow of drainage water, which would build up at this layer transition and spread out laterally.

Storm 1

INFILTRATION OF STORM WATER: **Figure 19** illustrates the distribution of saturation in the flow region for the first two hours of injection of the first storm. By the time of 0.5 hours of injection, water had already reached the layer transition at 30 feet and begun infiltrating into the second, less permeable layer. As the vertical flow was retarded by the abrupt decrease in permeability, horizontal flow took place along the material boundary. Over the time period of 0.25 to 0.5 hours of injection, the average rate of vertical flow was approximately 7.7 feet per hour. As in Case 1, the high initial rates of flow were due to the high pressure gradients that result when water under pressure is introduced into a relatively dry porous medium. By a time of 0.5 hours, flow rate in the vertical direction had decreased substantially.

The large decrease in vertical flow rate is largely due to the much lower hydraulic conductivity of the second layer of soil. Flow rate in the horizontal direction over this period also decreased, but not by nearly as much. Whereas average vertical flow rate decreased by about 4 times during this period, average horizontal flow rate decreased by about 1.5 times. This was due to the major part of the horizontal flow taking place in the uppermost layer of soil, where hydraulic conductivity is high. As in the first case, the rate of subsurface movement of flow continued to decrease throughout the period of injection of the first storm, approaching steady state rates over time. Some fluctuations in vertical and horizontal flow rates took place over this time, due to adjustments in the height of the water within the dry well in order to maintain the constant flow rate of about 0.5 cubic feet per second. Throughout the period of injection of the first storm, the saturated part of the drainage plume, delineated approximately by the contour of 95% saturation, continued to expand both in the horizontal and vertical directions. The contours of 50% and 75% saturation (s = 0.50 and 0.75, respectively) delineate portions of the unsaturated capillary fringe preceding the saturated portion of the drainage plume. The 50% saturation line extends across the width of the flow grid at a depth of 30 feet because the lower material happened to be at exactly 1/2 saturation when under the initial condition pressure head of -2.36 feet. By the time of 2.827 hours, when the 5,000 cubic feet of runoff water from the first storm had been completely injected, the 95% saturated portion of the drainage plume had reached points of about 20 feet below the bottom of the dry well and 27 feet in the horizontal direction from the center of the dry well (**Figure** 20a). The direction of flow for the drainage plume was primarily horizontal during this period.

DISTRIBUTION OF DRAINAGE PLUME: Although the volume of water injected through the dry well was exactly the same as for Case 1, the distribution of the drainage plume was quite different under the layered geologic conditions. Whereas in the first case injection water from the dry well reached the water table between 1.5 and 2.0 hours, the plume remained

56.25 feet above the water table at the end of the first storm in Case 2. In addition, the diameter of the plume was much larger, exposing the injection water to a much greater area of soil.

By performing a volume and soil particle surface area calculation below the dry well similar to that in Case 1, the specific soil surface contained within the maximum area of 80% saturation was calculated. The total specific surface of the soil particles to which drainage water was exposed in Case 2 was estimated to be 4.503878 x 10" square meters, about 16.2 times that for Case 1. Two main factors contributed to the greatly increased specific surface of vadose zone soil particles for Case 2: 1) the larger radius of the drainage plume, and 2) the larger specific surface of the finer soil particles constituting the second material. Furthermore, because the soil material below 30 feet was much less permeable than Material 1, the slower rate of infiltration allowed more time for adsorption to take place.

24-Hour Drainage Period

Figures **20b through 22a** illustrate the distribution of flow parameters for the 24-hour drainage period separating the two storms. These figures show the downward percolation and gradual dissipation of the saturated portion of the drainage plume left over from the first storm. During the first hour of drainage, the vertical flow rate of the saturated plume continued to diminish. Over the time periods extending from the end of the first storm to 0.25, 0.50 and 1.0 hours of drainage, the vertical flow rate was 3.78 feet per hour, 2.09 feet per hour and 1.766 feet per hour, respectively, judging from the progression of the zone under 95% saturation. From the time of 1.5 to 2.0 hours of drainage, the average vertical flow rate was 1.0 feet per hour. Figures **21b** and **22a** show little change in the plume configuration from 5.5 hours of drainage to 24 hours of drainage, indicating a very low rate of flow through the low-conductivity sandy clay loam material.

Storm 2

The vertical and horizontal movements of the drainage plume through the period of injection of the second storm were very similar to those of the first storm. Both horizontal and vertical flow rates were higher during this period due to the higher soil moisture in the area surrounding the dry well, a result of injection of water from the first storm. As a result, soils in the area around and below the dry well took on a higher hydraulic conductivity. As in the first storm, both horizontal and vertical rates of advance for the drainage plume decreased with time throughout the period of injection, though they remained consistently higher than in the first storm due to the higher background moisture. Between 1.25 hours and 1.75 hours of injection, average vertical flow rate was 7.7 feet per hour and average horizontal velocity was 4.7 feet per hour. By the time of 1.75 hours of injection, the contour of 95% saturation, moving progressively further down with the advance of the infiltration front, had nearly assimilated the small region of 95% saturation remaining in the soil below the dry well from the first storm (**Figure 23b**). By the time of 2.629 hours of injection, the time required to inject 5,000 cubic feet of water from the second storm, the saturated portion of the drainage plume had reached a point 45.8 feet above the water table, approximately 10.5 feet further down than it was at the end of injection from the first storm (**Figure 24a**). At this time the plume reached a distance horizontally from the center of the dry well along the layer transition of about 33.5 feet, only about a foot farther than it was after injection from the first storm. Thus, it appears that during the second storm, the proportion of vertical to horizontal flow of drainage water was greater than during the first storm. This may be attributed to the higher moisture content of the soil prior to injection, allowing for more vertical gravity drainage and resulting in less perched water at the layer transition and subsequent lateral flow.

Post-Storm 2 Drainage

Up until about two hours following the end of injection from the second storm, portions of this region remained saturated. Downward flow rate of the saturated portion of the plume averaged about two feet per hour during this time. Beyond approximately two hours following the second storm, the entire flow region was unsaturated, though a large portion of it remained in a state of 90-95% saturation up to a time of 130 hours following the second storm.

From a time of 9.0 hours to 286.0 hours following Storm 2, the slow, downward percolation of drainage water can be monitored through the movement of the saturation contours (**Figures 25 through 27**). From 3.0 hours following Storm 2 on, the zone of 90% saturation advanced at rates of less than one foot per hour. Between 84 and 130 hours following the second storm, the rate slowed to less than 0.1 foot per hour. By a time of 262 hours after the second storm, the contour of 80% saturation reached the water table (**Figure 27**). At a time of 286 hours following the storm, the distribution of saturation in the flow region had changed only slightly. Generally speaking, gravity drainage will continue at this slow rate until all of the water under 80% saturation has been assimilated into the aquifer. Given time, the water under 70% saturation will also be assimilated. Gravity drainage will continue until the soil reaches field capacity, whereupon negative pressure (suction) forces in the soil bind the water, and percolation rates become very small. **Figure 28a** illustrates the distribution of hydraulic head for the first storm of Case 2. The flow lines illustrate the effect of a horizontal component of flow developing at the layer transition at 30 feet over time. Flow moves laterally along the layer transition until it resumes a primarily vertical path of infiltration toward the water table, upon penetrating the clay loam layer. The flow paths shown at a time of 1.66 hours of injection from the first storm are essentially the same as those at the end of the injection period (**Figures 28b and 29a**). The flow paths observed at the end of the second storm show essentially the

same configuration as those at the end of the injection period for the first storm (Figure 29b).

CASE 3 SIMULATION

The distribution of soil saturation throughout the period of injection of a five-year, one-hour storm and subsequent drainage period in the third case is similar to both Cases 1 and 2, but represents an intermediate stage of moisture distribution in comparison to Cases 1 and 2. The saturated hydraulic conductivity of the soil material underlying the layer transition in this case was 1.0 foot per hour, less than that of the same zone for Case 1, and greater than that of the same zone for Case 2. As one would expect, some lateral migration of drainage water occurred at the layer transition, but not to the same degree as in the second case (Figures 30a through 30c). The rate of downward movement of drainage water to the water table following injection of storm water was higher than that for Case 2, due to the higher hydraulic conductivity of the soil material. The zone of 90% saturation contacted the water table some time between 3 and 5 hours, compared to over 130 hours in Case 2 (Figures 31c and 32a).

A volume and surface area calculation similar to that used in the other two cases was performed. The total surface area of soil particles to which drainage water is exposed in this case was estimated at 1.570927 x 10" square meters (Table 2), roughly 25 times that for Case 1, and slightly more than a third of that for Case 2.

The distribution of hydraulic head for the flow region during storm water injection for Case 3 illustrates the development of a horizontal component of flow with time, as in Case 2 (Figure 33). The flow paths do not extend outward radially as far as in Case 2, however, due to the higher hydraulic conductivity of the sandy loam below the layer transition.

The third simulation was terminated at the end of the 24-hour drainage period following injection of storm water from the first storm due to the development of a numerical problem with the computer program in the beginning stages of injection of water from the second storm. At this point, the computer program began to predict excessively high levels of water at the water table, inconsistent with the amounts of water that had been injected during the first storm. It is believed the problem was caused by some numerical instability associated with the unusually dry soil condition used as an initial condition for the model. Judging from the previous two cases, simulation of injection of storm water from only one storm is adequate for the assessment of flow rates, flow paths and exposure to soil particle surfaces in the vadose zone.

CONCLUSIONS

The direction of flow in Case 1 was primarily vertical. Vertical flow velocities were highest at the beginning of an injection event, and decreased steadily up until the time of contact with the regional aquifer. Contact of injection water with the regional aquifer was made between 1.5 and 2.0 hours of injection. The specific surface for the soil particles contained about 2.777514×10^{10} square meters. Vertical flow velocities were higher during injection from the second storm event than during injection from the first storm event, due to a higher initial degree of saturation and relative hydraulic conductivity. Contact of injection water with the regional aquifer was made between 15 minutes and 45 minutes of injection from the second event. The dimensions of the drainage plume remained essentially unchanged during the second storm injection event.

In Case 2, perching of injection water along the layer transition at 30 feet induced lateral components of flow along the layer transition. The 95% saturated portion of the drainage plume reached a maximum horizontal distance of about 27 feet from the center of the dry well during the first injection event. This distance increased to about 32 feet during the second injection event. The time required for the 90% saturated portion of the drainage plume from both injection events to reach the regional water table was between 130 and 150 hours. The specific surface of soil particles included in the largest area of 80% saturation during the simulation was about 4.503878 x 10" square meters.

Horizontal flow occurred along the layer transition during injection events for Case 3 also, but to a lesser extent than in Case 2. The maximum extent of horizontal movement of the 95% saturated portion of the drainage plume during the first injection event was about 21.5 feet from the center of the dry well. Vertical flow velocities of injection water were lower than in Case 1 and higher than in Case 2. Injection water from the first event contacted the regional aquifer between 5.5 hours and 6.25 hours after the start of injection. Specific surface area of soil particles included

within the maximum extent of the zone of 80% saturation was about 1.570927 x 10" square meters.

RECOMMENDATIONS

1. Dry wells should not be placed in areas where subsurface conditions are characterized by uniform, highly permeable soil materials between the dry well and the water table. Drainage via dry wells into this type of subsurface environment allows for a minimum of attenuation of water-borne pollutants in the vadose zone.

2. Dry wells should be placed in areas where subsurface conditions are characterized by multi-layered soil materials, some of which are predominantly clay in composition. Drainage via dry wells into this type of subsurface environment allows for a maximum of attenuation of water-borne pollutants in the vadose zone.

3. Strict regulation of the location of dry wells and of all materials entering dry wells should be applied. The distance of about 75 feet between the bottom of the dry well and the water table assumed in this study is sufficient for some attenuation of pollutants in the drainage water to take place. However, even under the most favorable subsurface conditions, attenuation of contaminants in the vadose zone may be incomplete.

REFERENCES

Bandeen, R. F., 1984. **Case Study Simulations of Dry Well Recharge in the Tucson Basin.** Completion Report to Pima County Department of Transportation and Flood Control District.

Bouwer, H., and R. C. Rice, 1984. "Hydraulic Properties of Stony Vadose Zones," **Ground Water**, Vol. 22, No. 6.

Buckman, H. O., and N. C. Brady, 1969. **The Nature and Properties of Soils.** Macmillan, New York, 1969.

Coelho, M. A., 1974. **Spatial Variability of Water Related Soil Physical Properties.** Ph.D. Dissertation, University of Arizona, Tucson, Arizona.

Davis, L. A., and S. P. Neuman, 1983. **Documentation and User's Guide: UNSAT 2 - Variably Saturated Flow Model.** Water, Waste and Land, Inc. Prepared for the U.S. Nuclear Regulatory Commission, NUREG/CR-3990, WWL/TM-1791-1.

De Tommasso, S.C., McGuckin Drilling, Inc., Phoenix, Arizona, June 1984. **Personal Communication.**

Dumeyer, J. M., 1966. **Stratigraphy and Hydrogeology of the Water Resources Research Center Recharge Area.** Unpublished Report, University of Arizona, Department of Hydrology, Tucson, Arizona.

Feddes, R. A., E. Bresler, and S. P. Neuman, 1974. **Field Test of a Modified Numerical Model for Water Uptake by Root Systems.** Water Resources Research, 10(6): pp. 1199-1206.

Guma'a, G. S., 1978. **Spatial Variability of In-Situ Available Water.** Unpublished Ph.D. Dissertation, University of Arizona, Tucson, Arizona.

Hillel, Daniel, 1971. **Soil and Water, Physical Principles and Processes.** Academic Press, New York, San Francisco, London.

Kirkham, D., and W. Powers, 1984. **Advanced Soil Physics.** R. E. Krieger Company, Malabar, Florida, 1984.

Kroszynski, U. I., and G. Dagan, 1975. **Pumping in Unconfined Aquifers: the Influence of the Unsaturated Zone.** Water Resources Research, 11(3): pp. 479-490.

Neuman, S. P., R. A. Feddes, and E. Bresler, 1974. **Finite Element Simulation of Flow in Saturated-Unsaturated Soils Considering Water Uptake by Plants.** Development of Methods, Tools and Solutions for Unsaturated Flow. Third Annual Report. Technion, Haifa, Israel.

Neuman, S. P., 1975. **Galerkin Approach to Saturated-Unsaturated Flow in Porous Media.** Chapter 10 in Finite Elements in Fluids. Vol. I: Viscous Flow and Hydrodynamics. Edited by R. H. Gallagher, J. T. Oden, and O. C. Zienkiewicz. John Wiley and Sons, London. pp. 201-217.

Osborne, P. S., 1969. **Analysis of Well Losses Pertaining to Artificial Recharge.** Master's thesis, University of Arizona, Tucson, Arizona.

Richards, L. A., 1931. **Capillary Conduction of Liquids in Porous Mediums.** Physics, 1, pp. 318-333.

U.S. Department of Agriculture, Soil Conversation Service and Forest Service, 1979. **Soil Survey of Santa Cruz and Parts of Cochise and Pima Counties, Arizona.**

U.S. Department of Interior, 1977. **Groundwater Manual.** Water Resources Technical Publication. U.S. Government Printing Office.

Van Genuchten, R., 1978. **Calculating Unsaturated Hydraulic Conductivity with a Closed-form Analytical Model.** U. S. Salinity Laboratory, U. S. Department of Agriculture, Riverside, California.

Wei, C. Y., and W. Y. Shieh, 1979. **Transient Seepage Analysis of Guri Dam.** Jour. Tech. Council ASCE 105(TCI), pp. 135-147.

White, R. E., 1979. **Introduction to Principles and Practice of Soil Science.** Wiley and Sons, New York.

Wilson, L. G., 1983. **A Case Study of Dry Well Recharge.** Water Resources Research Center, University of Arizona, Tucson, Arizona.

Wilson, L. G., 1986. **Effects of Channel Stabilization in Tucson Stream Reaches on Infiltration and Ground Water Recharge.** Draft final report to Pima County Department of Transportation and Flood Control District.

Zaslavski, D. and G. Sinai, 1981. **Surface Hydrology: In-surface Transient Flow.** Jour. Hydr. Div. ASCE 107 (HYI), pp. 65-93.

TABLE 1

REPRESENTATIVE VALUES OF SOIL BULK DENSITY AND SPECIFIC SURFACE

Soil Type (Material)	Bulk Density[1] (g/cm^3)	Specific Surface[2] (m^2/g)
Coarse Sand (Material 1)	1.5	0.01
Sandy Clay Loam (Material 2)	1.0	1.0
Sandy Loam (Material 3)	1.25	0.1

[1] After Buckman and Brady, 1969.

[2] After White, 1979.

TABLE 2

ESTIMATED SPECIFIC SURFACE OF SOIL EXPOSED TO DRY WELL DRAINAGE WATER

Case	Estimated Specific Surface (m^2)
1	12,284,300
2	5,954,513,338
3	328,875,897

Specific Surface Ratio:

Case 1: Case 2: Case 3 = 1:485:27

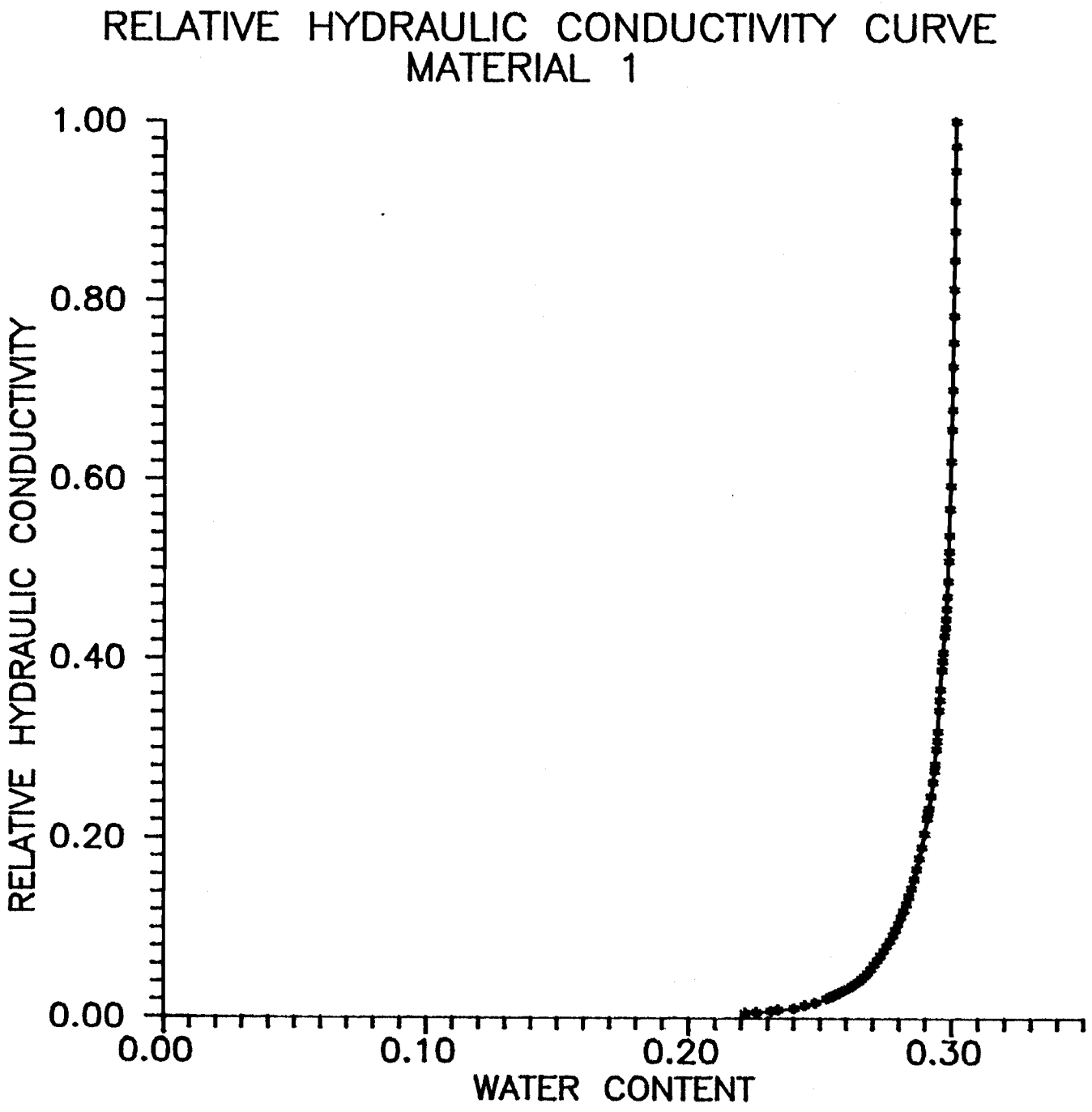
RELATIVE HYDRAULIC CONDUCTIVITY CURVE
MATERIAL 1
RELATIVE HYDRAULIC CONDUCTIVITY
1.00
0.80
0.60
0.40
0.20
0.00
0.00
0.10
0.20
0.30
WATER CONTENT

FIGURE 1

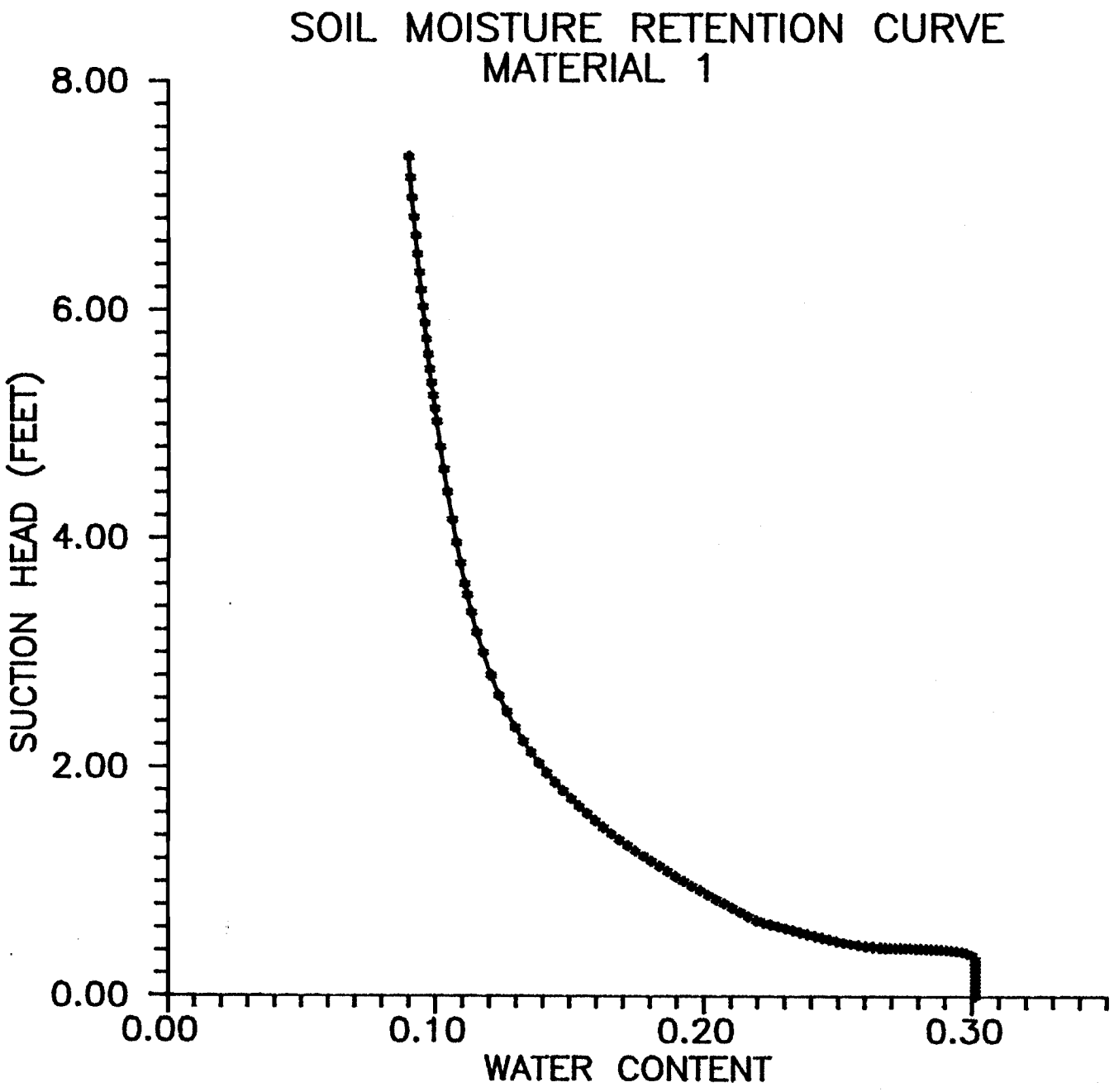
SOIL MOISTURE RETENTION CURVE
MATERIAL 1
8.00
6.00
4.00
2.00
0.00
SUCTION HEAD (FEET)
0.00
0.10
0.20
0.30
WATER CONTENT

FIGURE 2

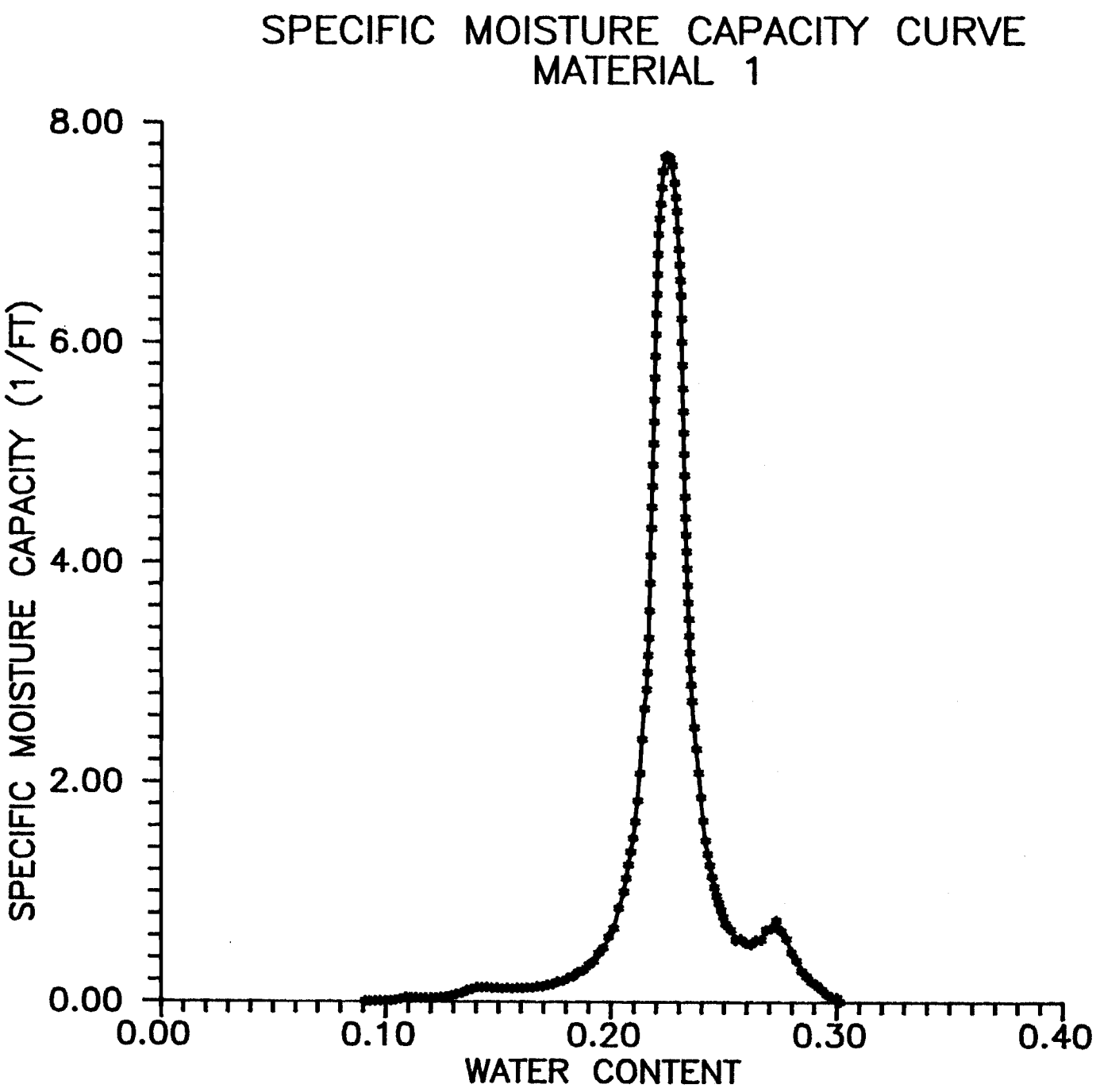
SPECIFIC MOISTURE CAPACITY CURVE
MATERIAL 1
SPECIFIC MOISTURE CAPACITY (1/FT)
8.00
6.00
4.00
2.00
0.00
0.00
0.10
0.20
0.30
0.40
WATER CONTENT

FIGURE 3

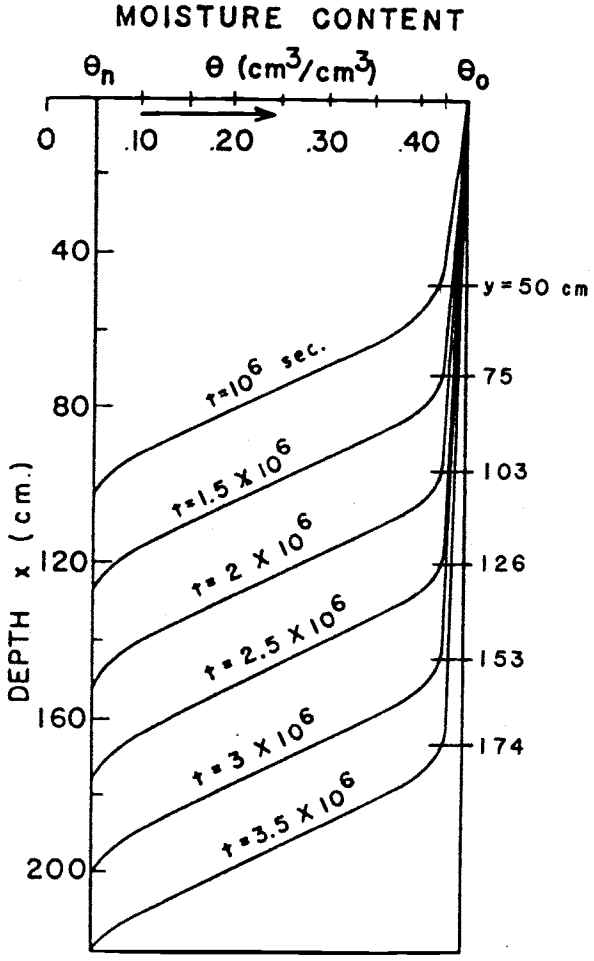

FIGURE 4.

DISTRIBUTION OF WATER CONTENT WITH DEPTH DURING VERTICAL INFILTRATION (after Kirkham and Powers, 1984)

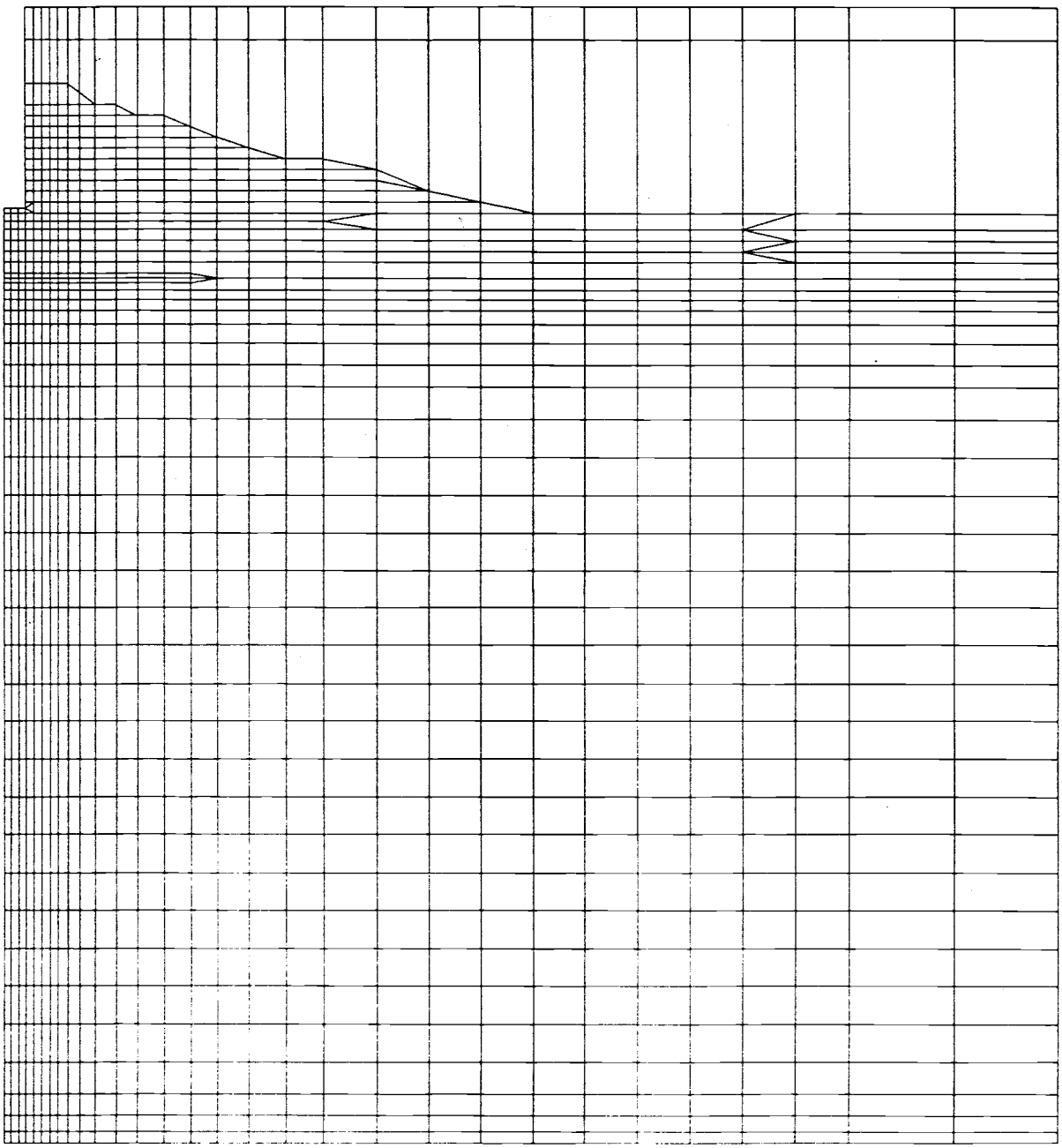

FIGURE 5

FINITE ELEMENT GRID

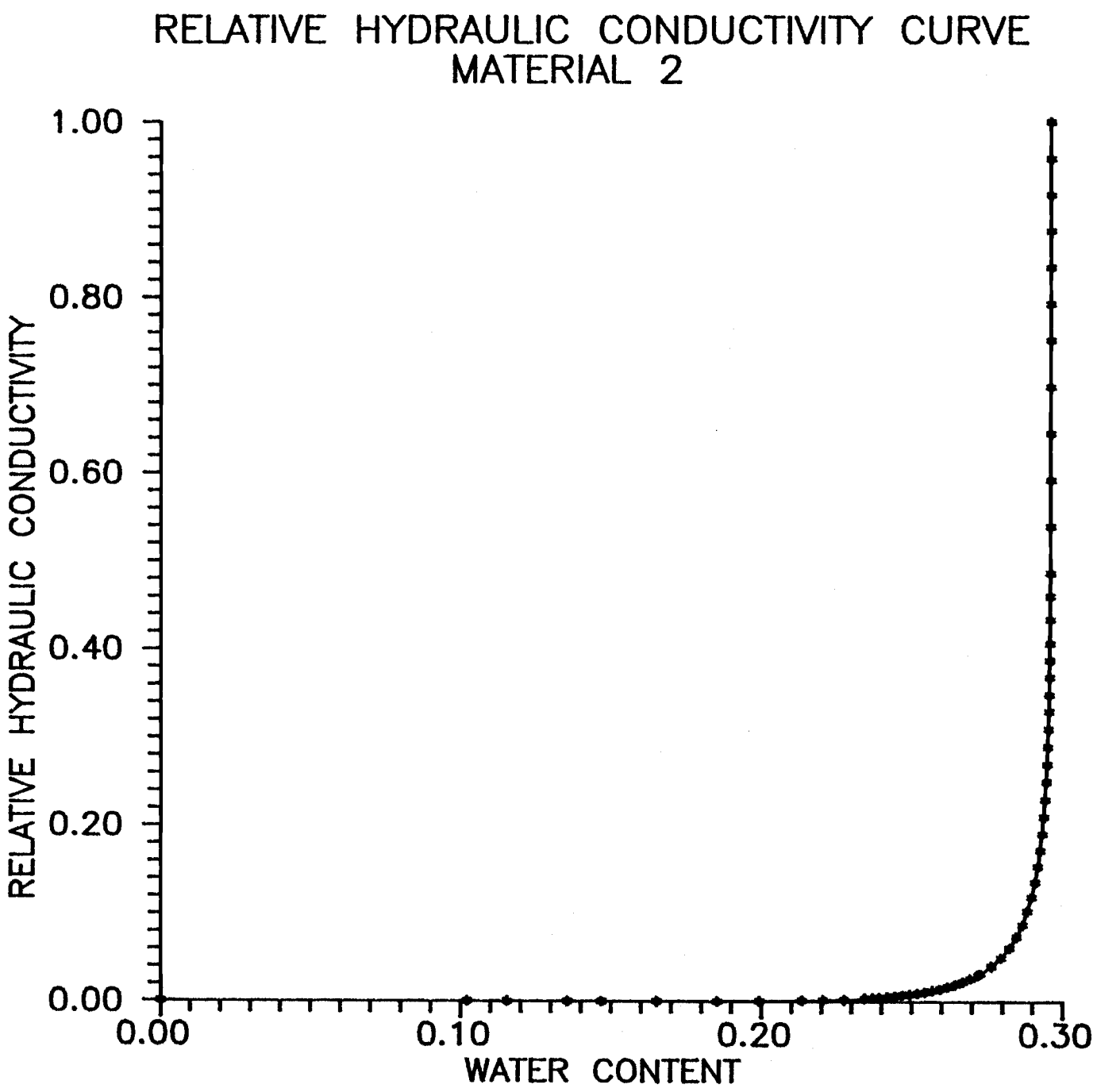
RELATIVE HYDRAULIC CONDUCTIVITY CURVE
MATERIAL 2
RELATIVE HYDRAULIC CONDUCTIVITY
1.00
0.80
0.60
0.40
0.20
0.00
0.00
0.10
0.20
0.30
WATER CONTENT

FIGURE 6

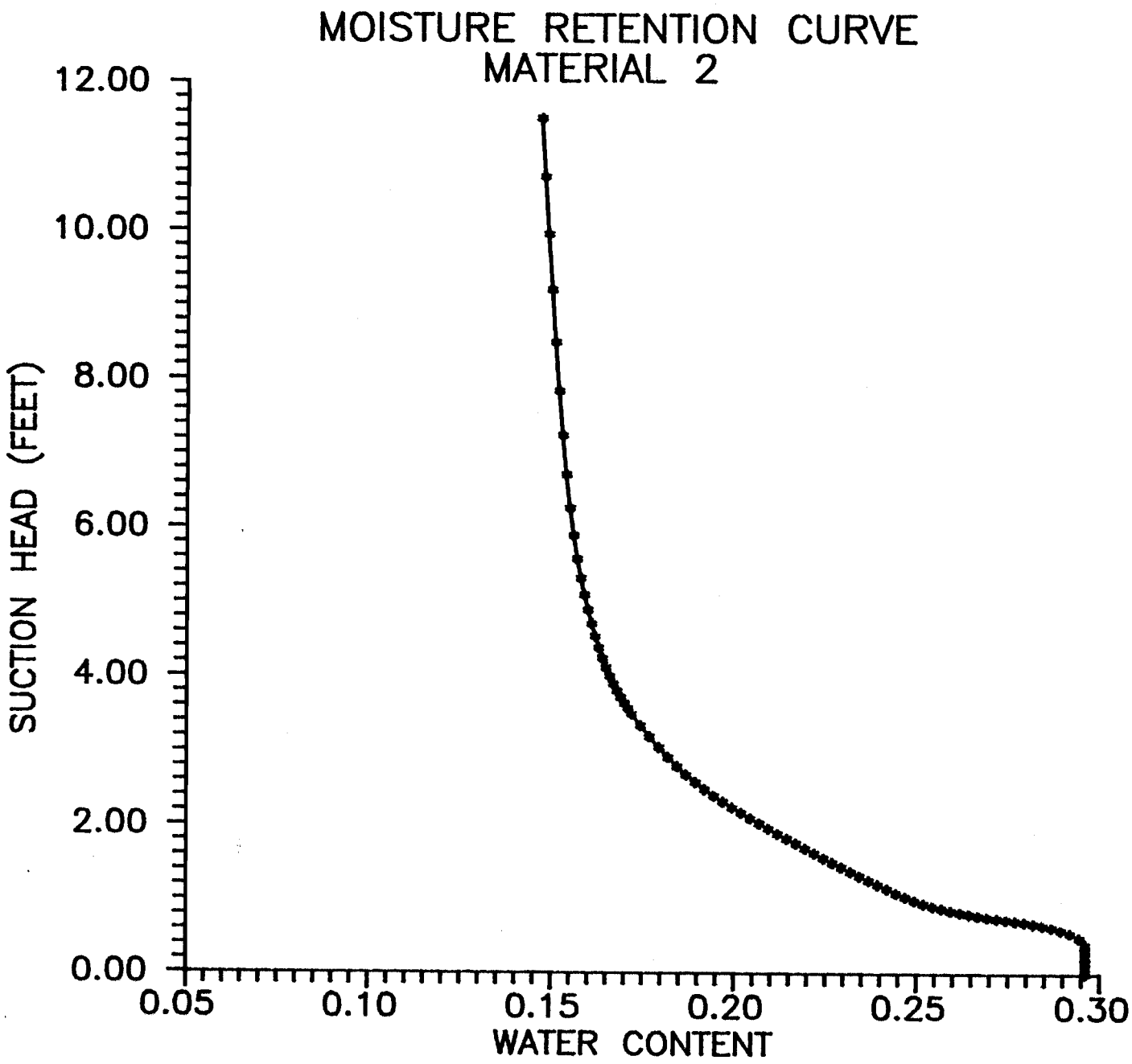
MOISTURE RETENTION CURVE
MATERIAL 2
SUCTION HEAD (FEET)
12.00
10.00
8.00
6.00
4.00
2.00
0.00
0.05
0.10
0.15
0.20
0.25
0.30
WATER CONTENT

FIGURE 7

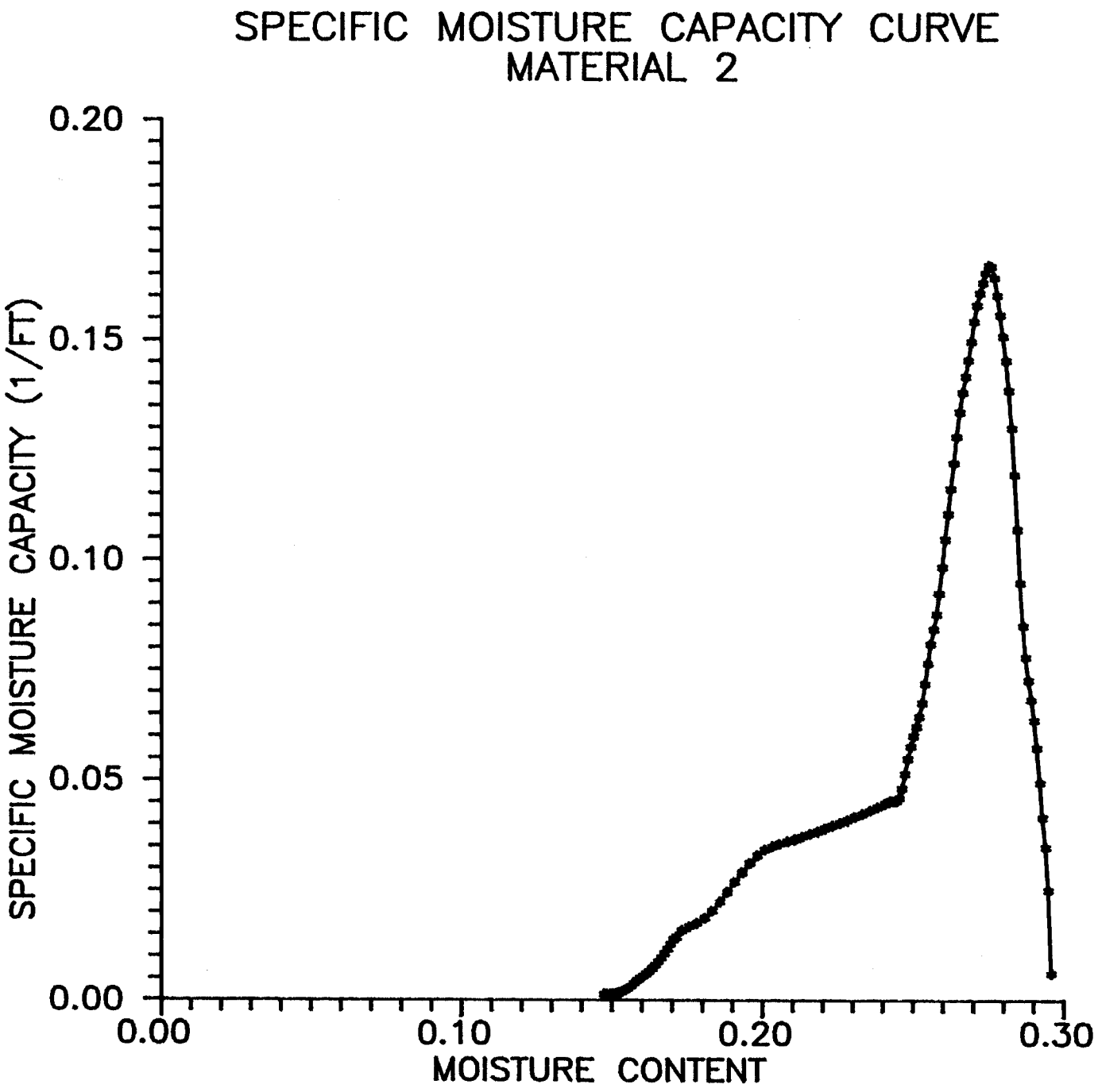
SPECIFIC MOISTURE CAPACITY CURVE
MATERIAL 2
SPECIFIC MOISTURE CAPACITY (1/FT)
0.20
0.15
0.10
0.05
0.00
0.00
0.10
0.20
0.30
MOISTURE CONTENT

FIGURE 8

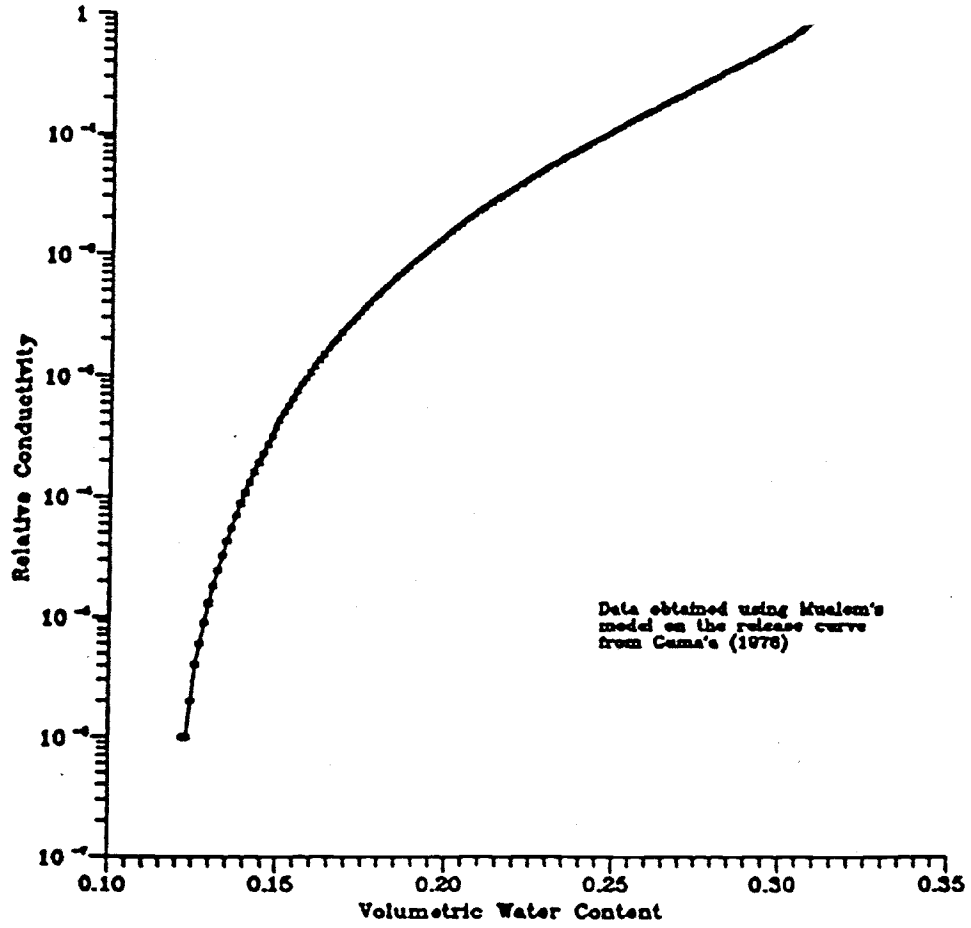

RELATIVE HYDRAULIC CONDUCTIVITY CURVE

MATERIAL 3

FIGURE 9 (after Wilson and Neuman, et. al., 1986)

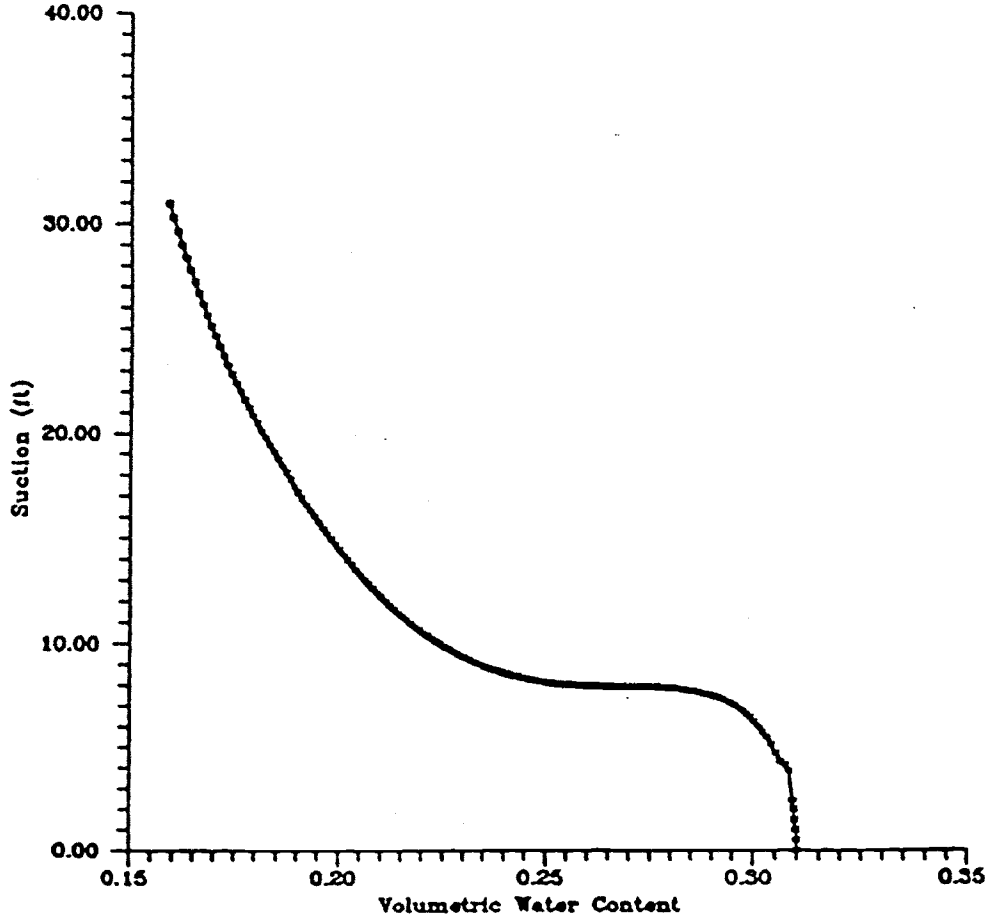

MOISTURE RETENTION CURVE

MATERIAL 3

FIGURE 10 (after Wilson and Neuman, et. al., 1986)

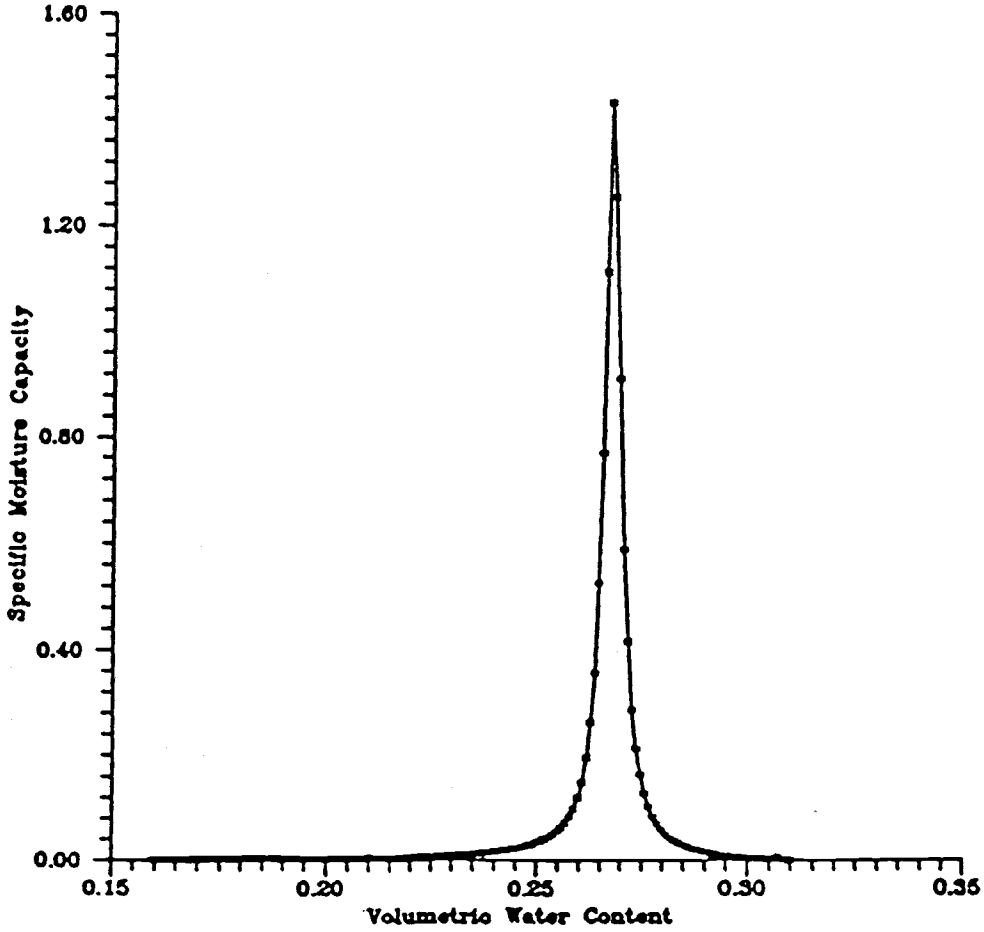

SPECIFIC MOISTURE CAPACITY CURVE

MATERIAL 3

FIGURE 11 (after Wilson and Neuman, et. al., 1986)

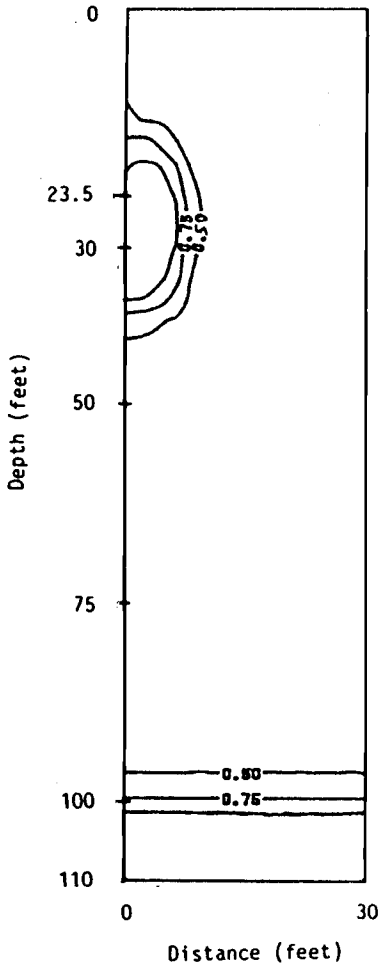

DEGREE OF SATURATION
0.250 HOURS OF INJECTION
CASE 1; STORM 1

Fig. 12a

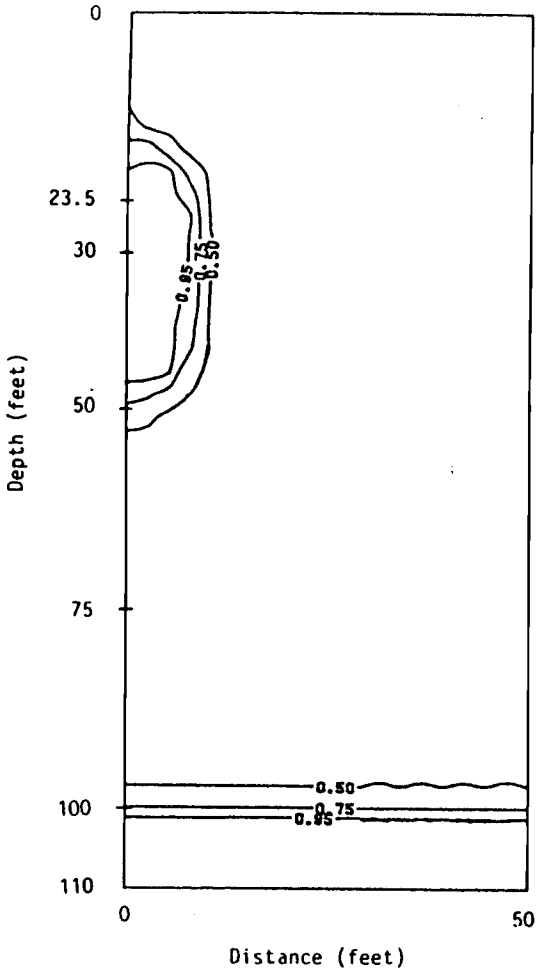

DEGREE OF SATURATION
0.500 HOURS OF INJECTION
CASE 1; STORM 1

Fig. 12b

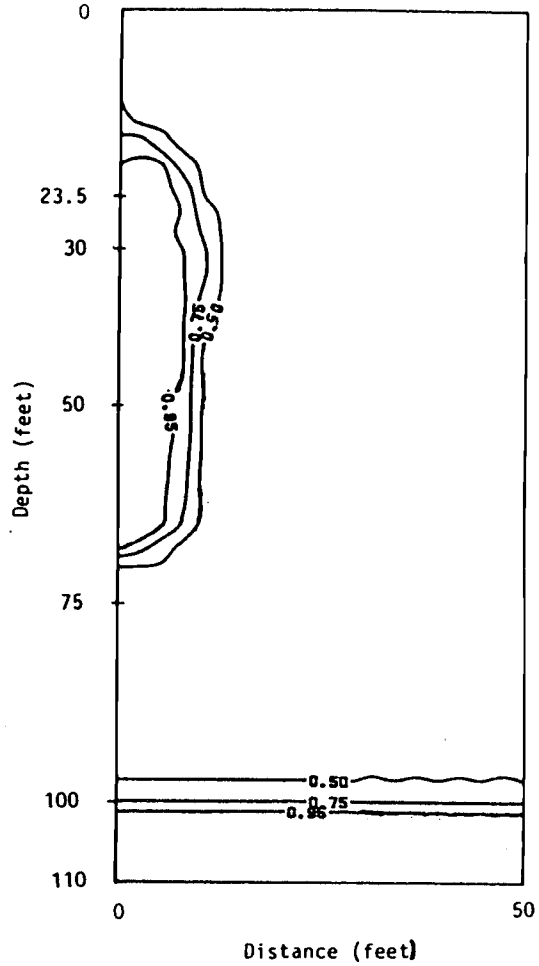

DEGREE OF SATURATION
1.000 HOURS OF INJECTION
CASE 1; STORM 1

Fig. 12c

FIGURE 12

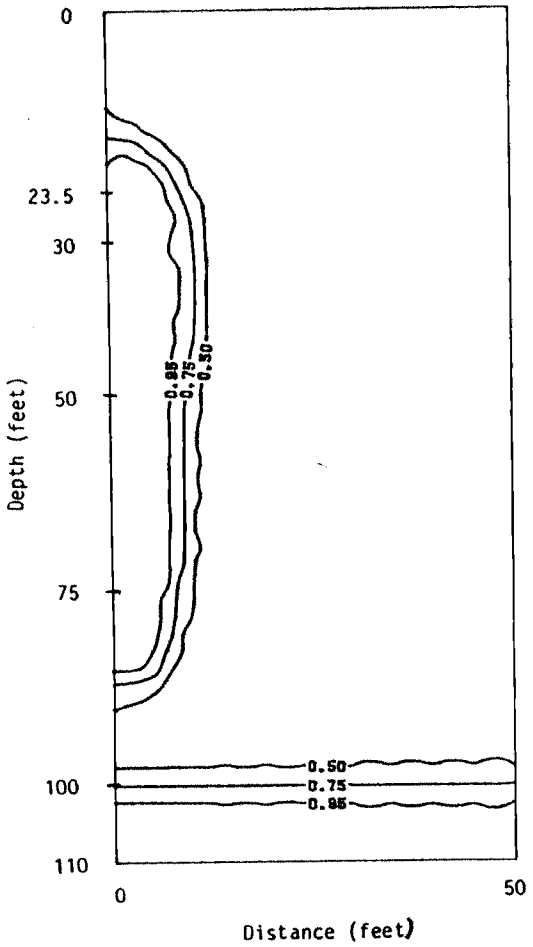

DEGREE OF SATURATION
1.500 HOURS OF INJECTION
CASE 1; STORM 1

Fig. 13a

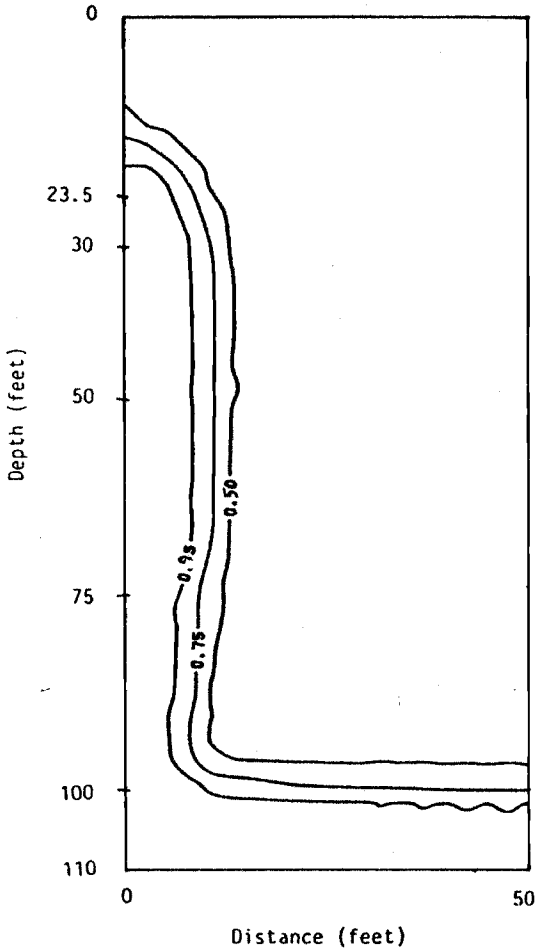

DEGREE OF SATURATION
2.72 HOURS OF INJECTION - 5000 CU. FT.
CASE 1; STORM 1

Fig. 13b

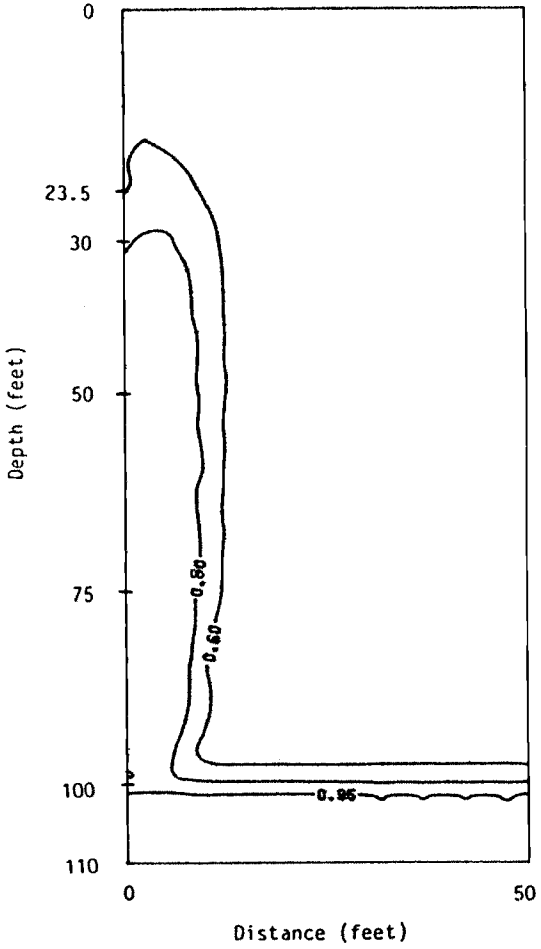

DEGREE OF SATURATION
2.0 HOURS POST-STORM 1 DRAINAGE
CASE 1; 4.722 HOURS TOTAL TIME

Fig. 13c

FIGURE 13

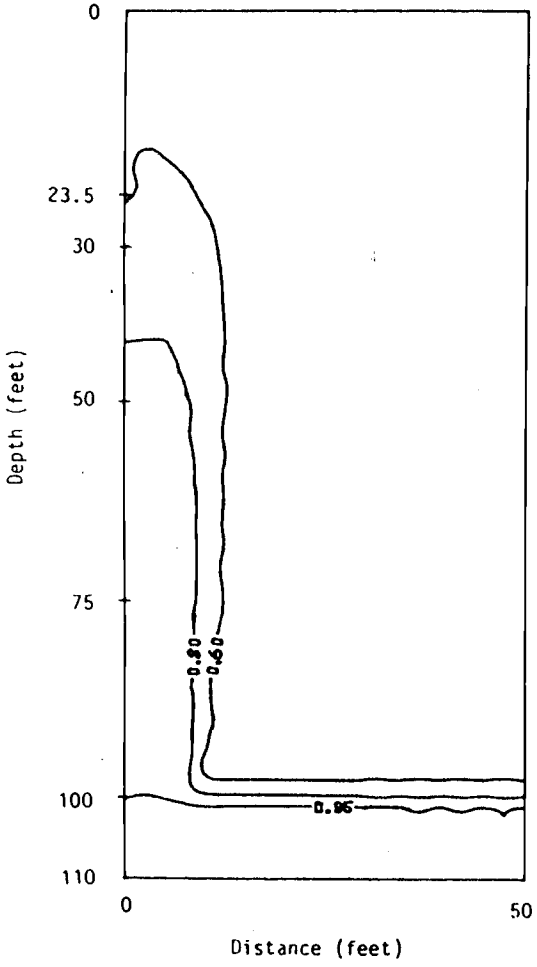

DEGREE OF SATURATION
5.0 HOURS POST-STORM 1 DRAINAGE
CASE 1: 7.722 HOURS TOTAL TIME

Fig. 14a

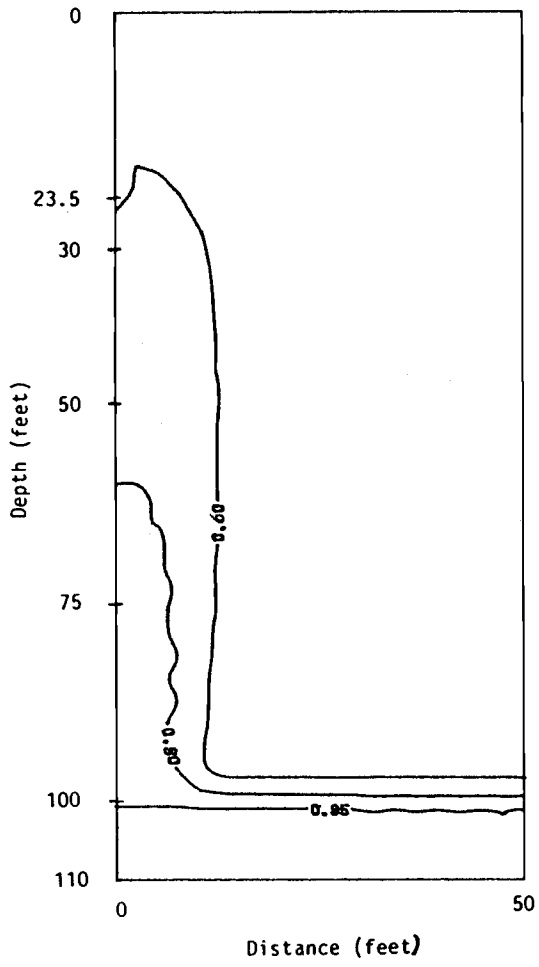

DEGREE OF SATURATION
9.0 HOURS POST-STORM 1 DRAINAGE
CASE 1: 11.722 HOURS TOTAL TIME

Fig. 14b

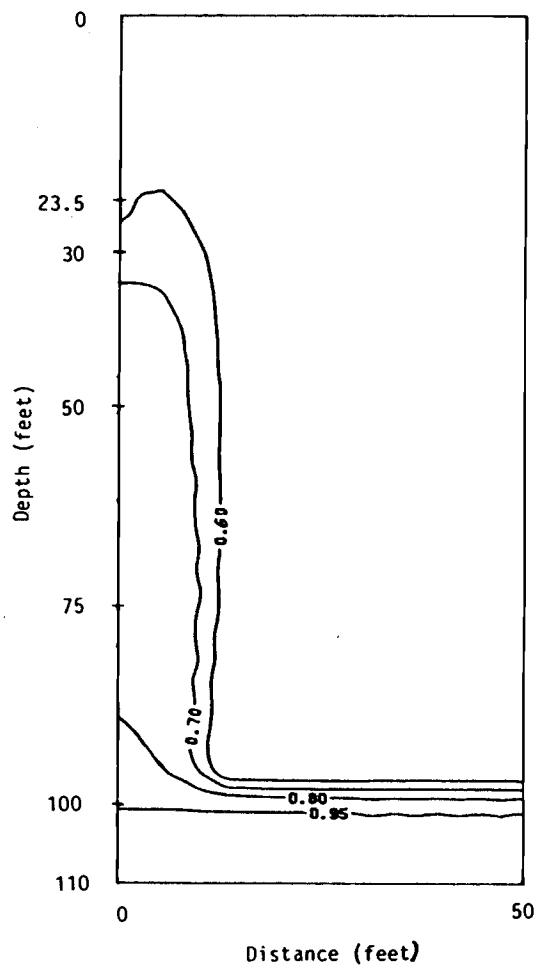

DEGREE OF SATURATION
15.0 HOURS POST-STORM 1 DRAINAGE
CASE 1: 17.722 HOURS TOTAL TIME

Fig. 14c

FIGURE 14

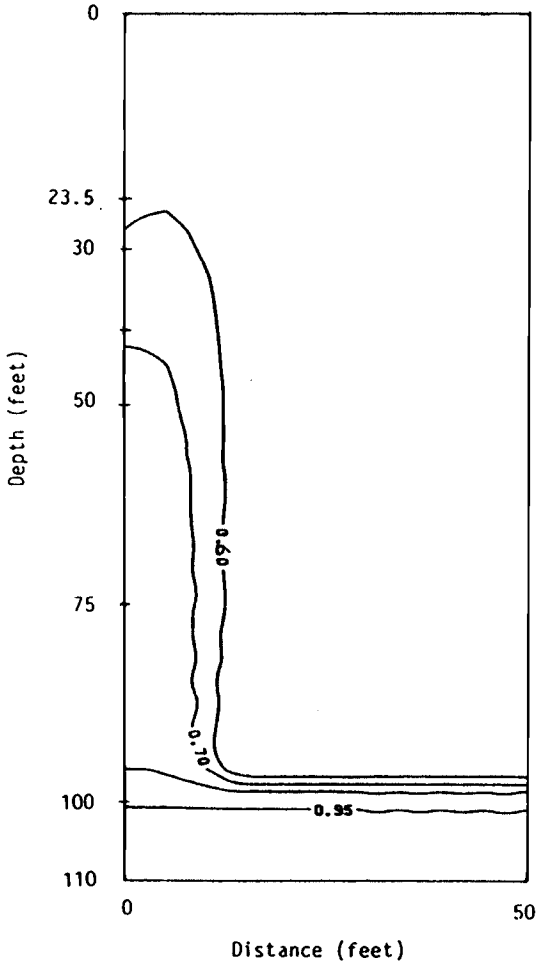

DEGREE OF SATURATION
24.0 HOURS POST-STORM 1 DRAINAGE
CASE 1: 26.722 HOURS TOTAL TIME

Fig. 15a

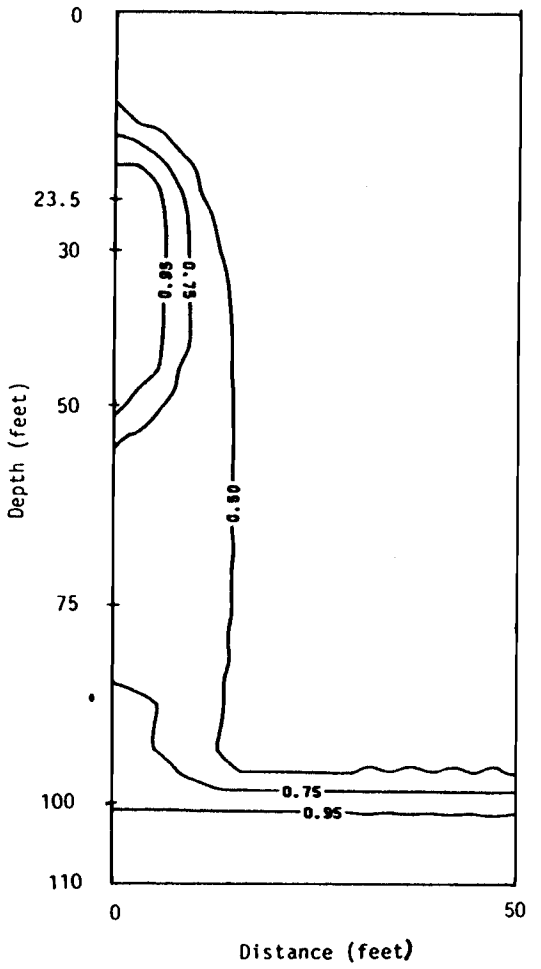

DEGREE OF SATURATION
0.250 HOURS OF INJECTION: STORM 2
CASE 1: 26.972 HOURS TOTAL TIME

Fig. 15b

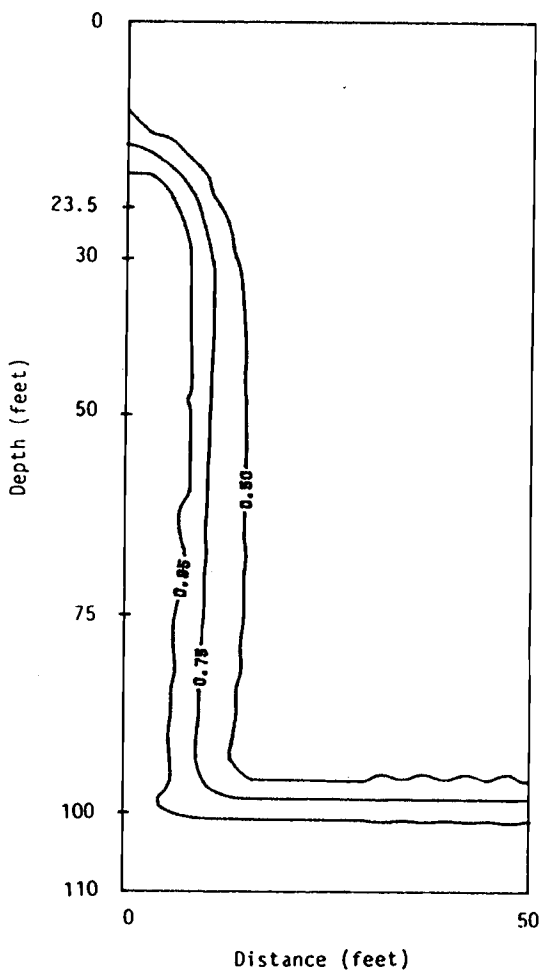

DEGREE OF SATURATION
0.750 HOURS OF INJECTION: STORM 2
CASE 1: 27.472 HOURS TOTAL TIME

Fig. 15c

FIGURE 15

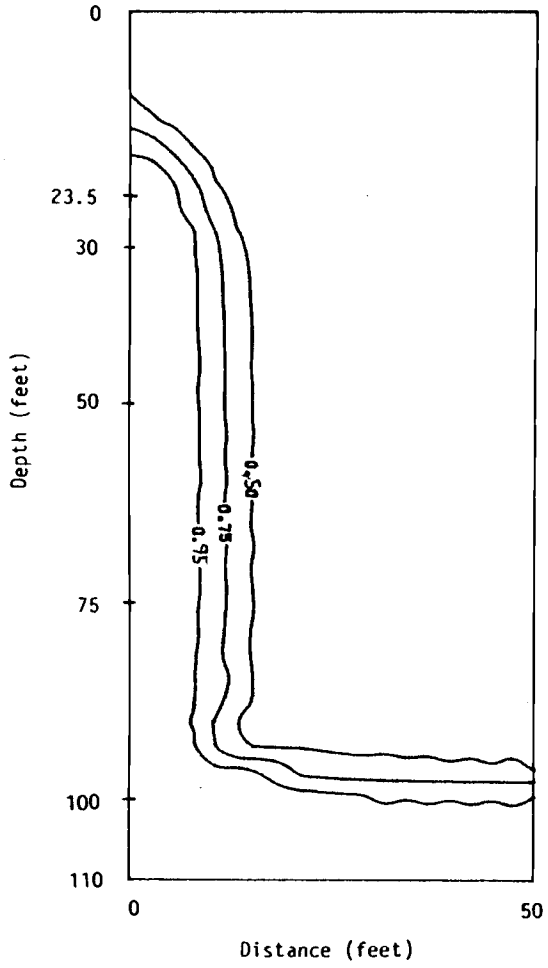

DEGREE OF SATURATION
2.663 HOURS OF INJECTION: STORM 2
CASE 1: 29.385 HOURS TOTAL TIME

Fig. 16a

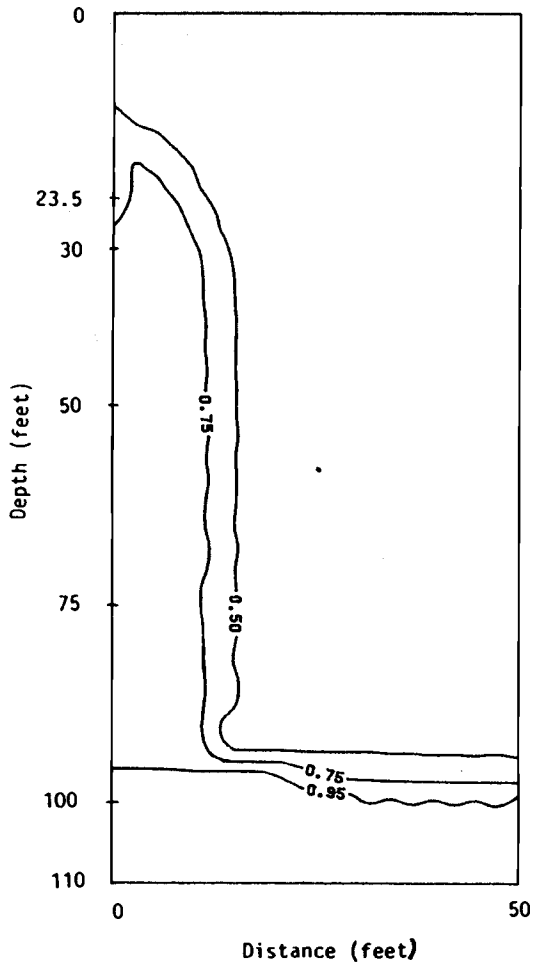

DEGREE OF SATURATION
0.50 HOURS POST-STORM 2 DRAINAGE
CASE 1: 29.885 HOURS TOTAL TIME

Fig. 16b

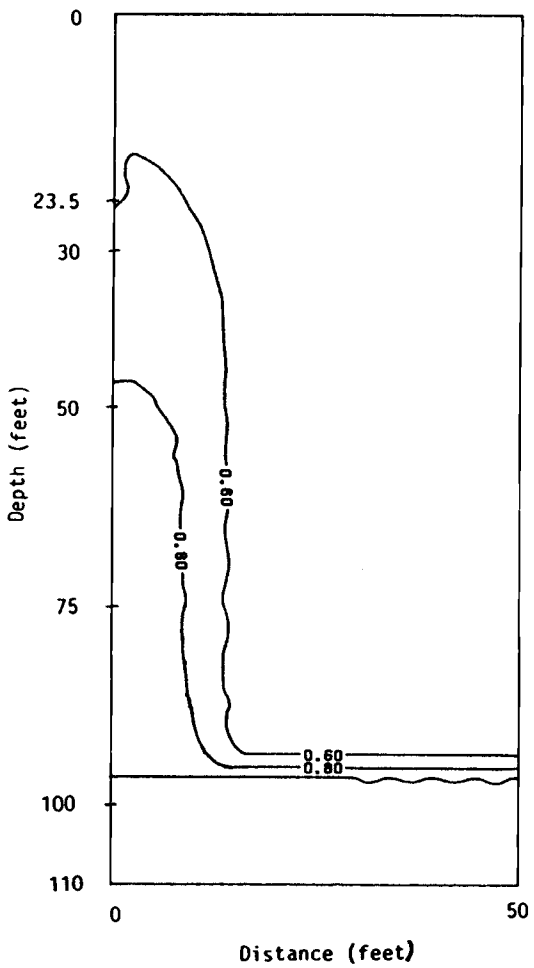

DEGREE OF SATURATION
6.00 HOURS POST-STORM 2 DRAINAGE
CASE 1: 35.385 HOURS TOTAL TIME

Fig. 16c

FIGURE 16

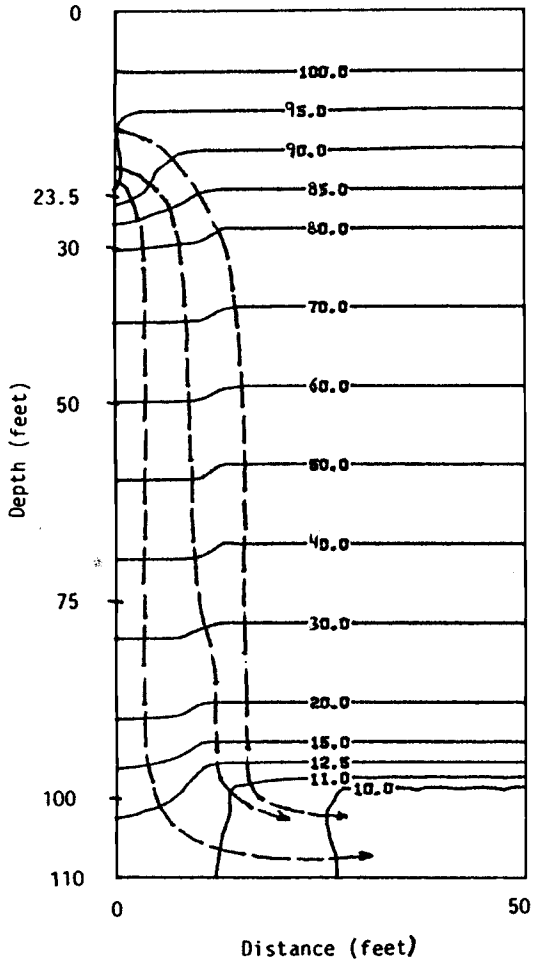

HYDRAULIC HEAD DISTRIBUTION (FEET)
2.72 HOURS OF INJECTION - 5000 CU. FT.
CASE 1; STORM 1

Fig. 17a

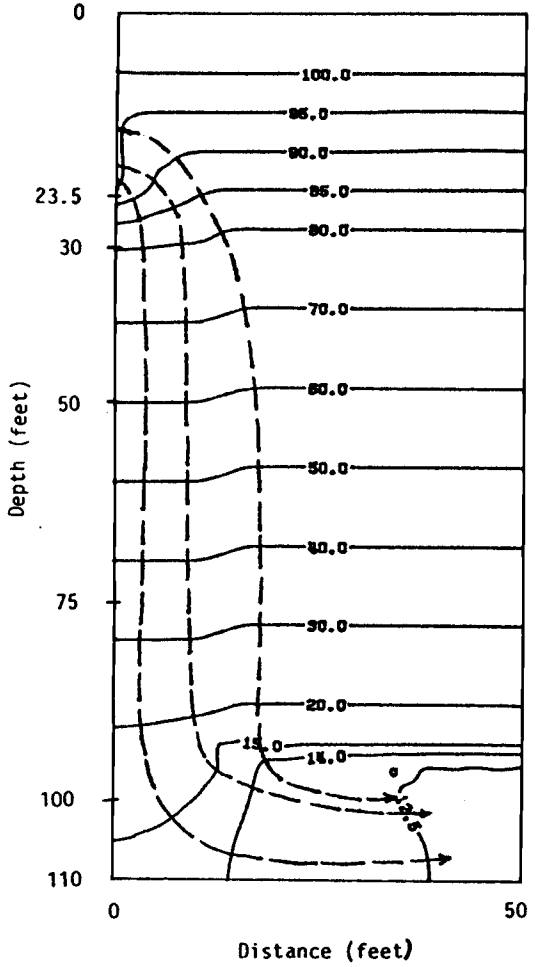

HYDRAULIC HEAD DISTRIBUTION (FEET)
2.663 HOURS OF INJECTION ; STORM 2
CASE 1: 29.385 HOURS TOTAL TIME

Fig. 17b

FIGURE 17

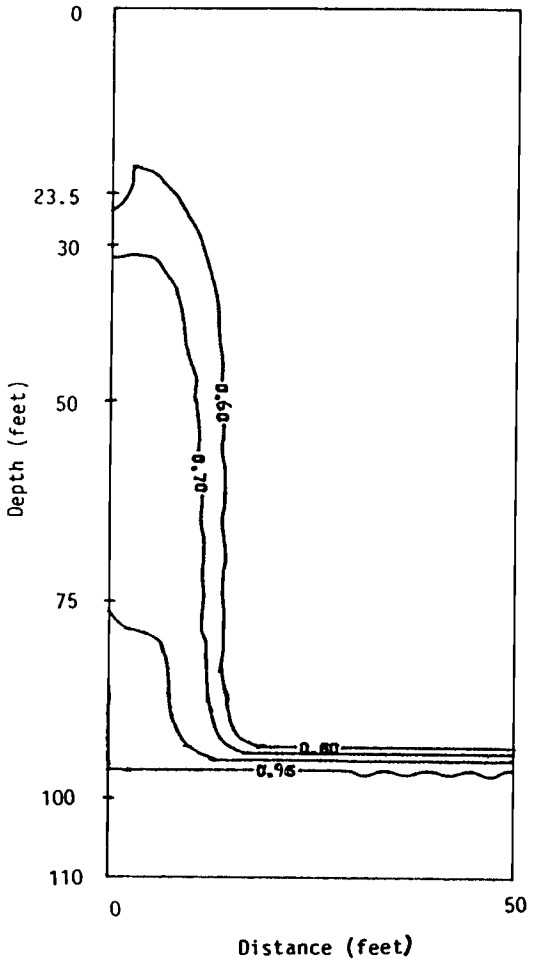

DEGREE OF SATURATION
12.00 HOURS POST-STORM 2 DRAINAGE
CASE 1: 41.385 HOURS TOTAL TIME

Fig. 18a

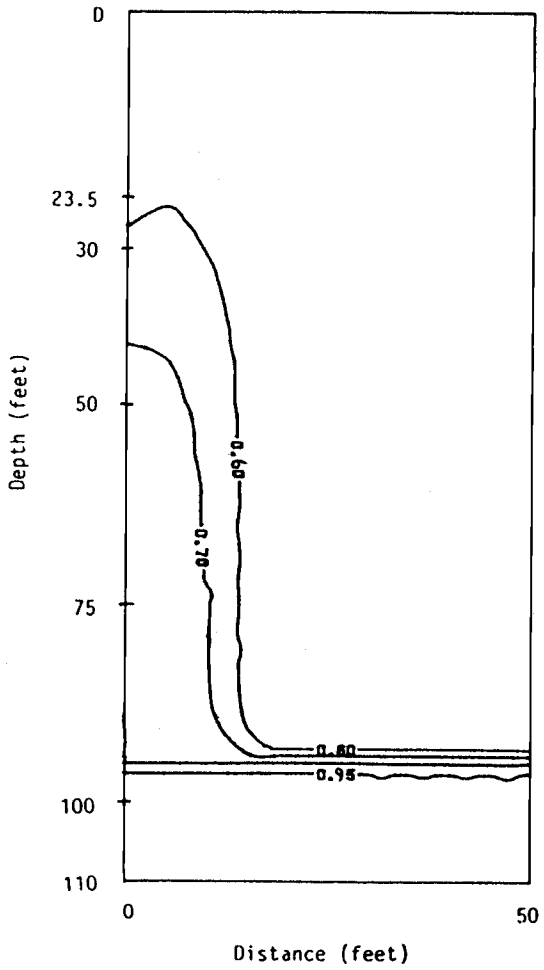

DEGREE OF SATURATION
24.00 HOURS POST-STORM 2 DRAINAGE
CASE 1: 53.385 HOURS TOTAL TIME

Fig. 18b

FIGURE 18

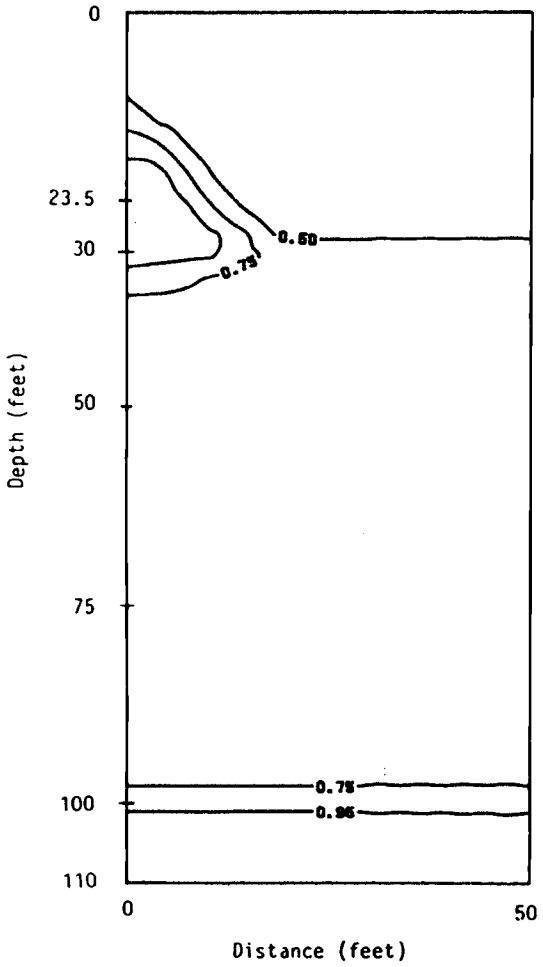

DEGREE OF SATURATION
0.50 HOURS OF INJECTION
CASE 2; STORM 1

Fig. 19a

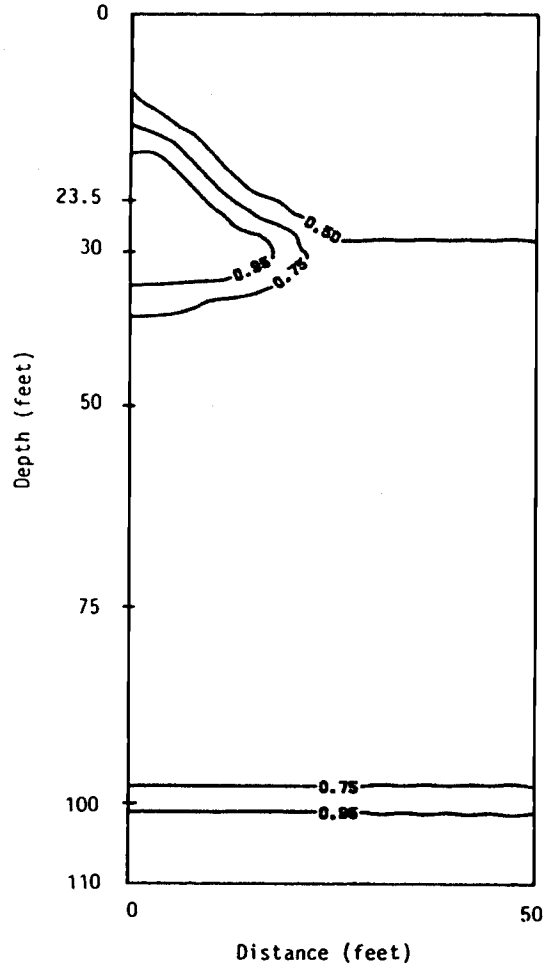

DEGREE OF SATURATION
1.00 HOURS OF INJECTION
CASE 2; STORM 1

Fig. 19b

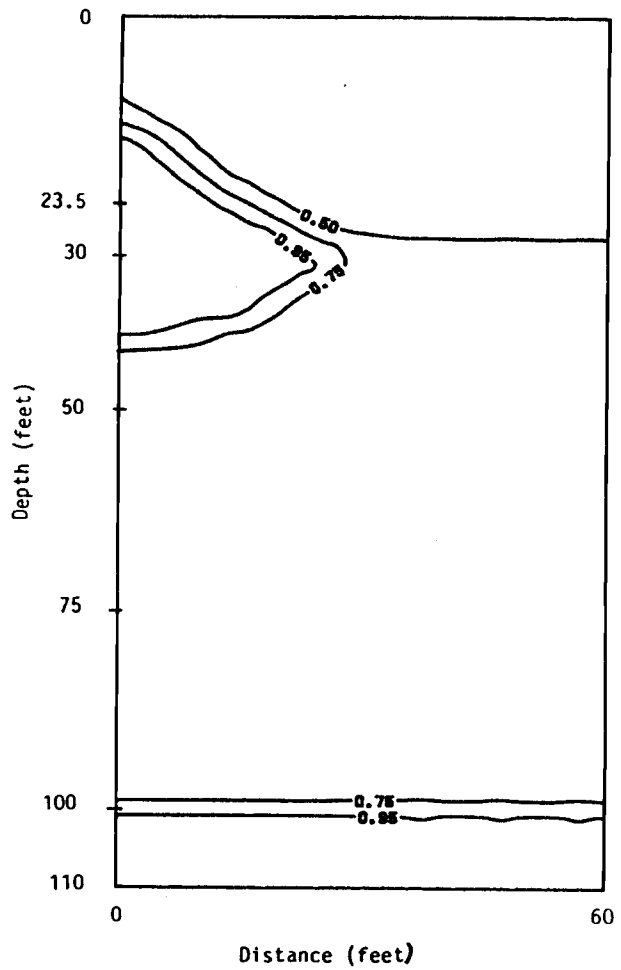

DEGREE OF SATURATION
2.00 HOURS OF INJECTION
CASE 2; STORM 1

Fig. 19c

FIGURE 19

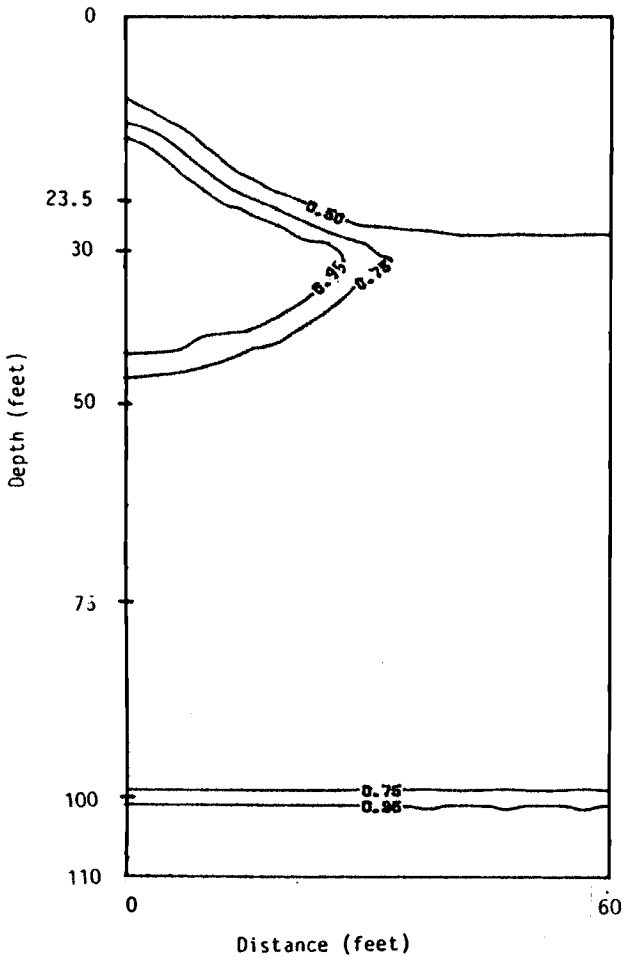

DEGREE OF SATURATION
2.827 HOURS OF INJECTION -
5000 CU. FT
CASE 2; STORM 1

Fig. 20a

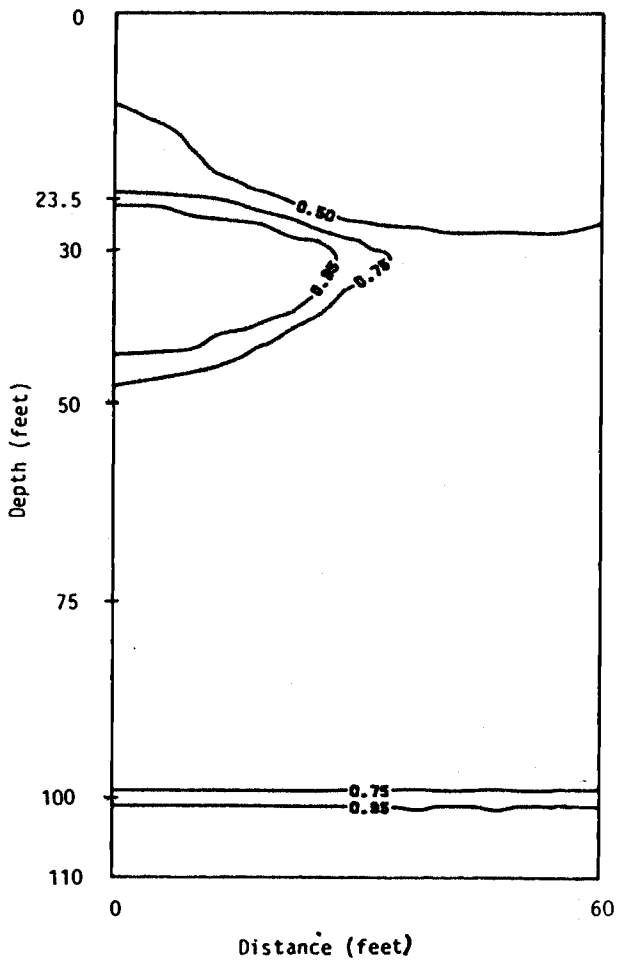

DEGREE OF SATURATION
0.25 HOURS OF POST-STORM 1 DRAINAGE
CASE 2: 3.077 HOURS TOTAL TIME

Fig. 20b

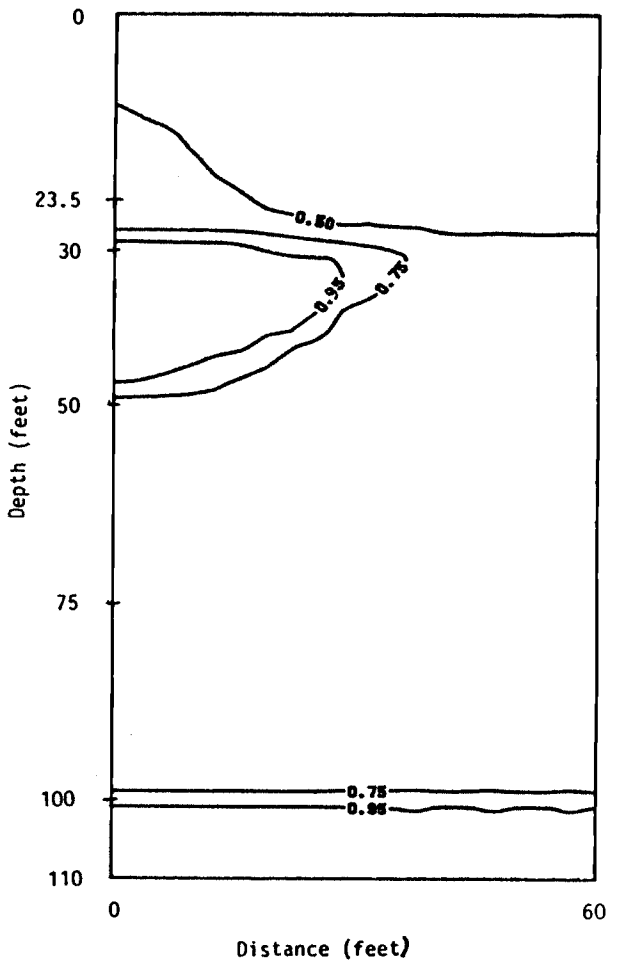

DEGREE OF SATURATION
1.00 HOURS OF POST-STORM 1 DRAINAGE
CASE 2: 3.827 HOURS TOTAL TIME

Fig. 20c

FIGURE 20

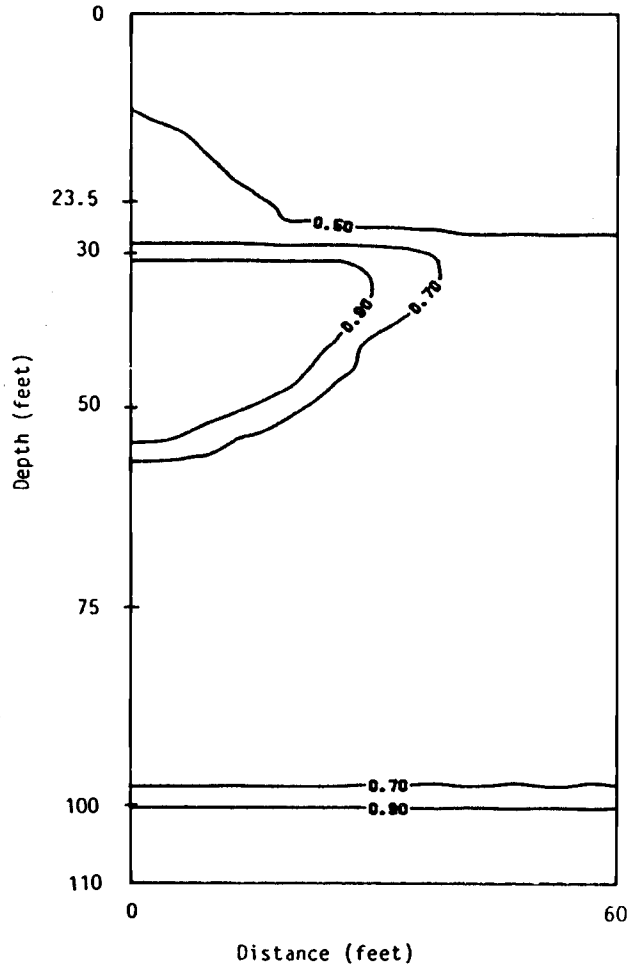

DEGREE OF SATURATION
4.00 HOURS OF POST-STORM 1 DRAINAGE
CASE 2: 6.827 HOURS TOTAL TIME

Fig. 21a

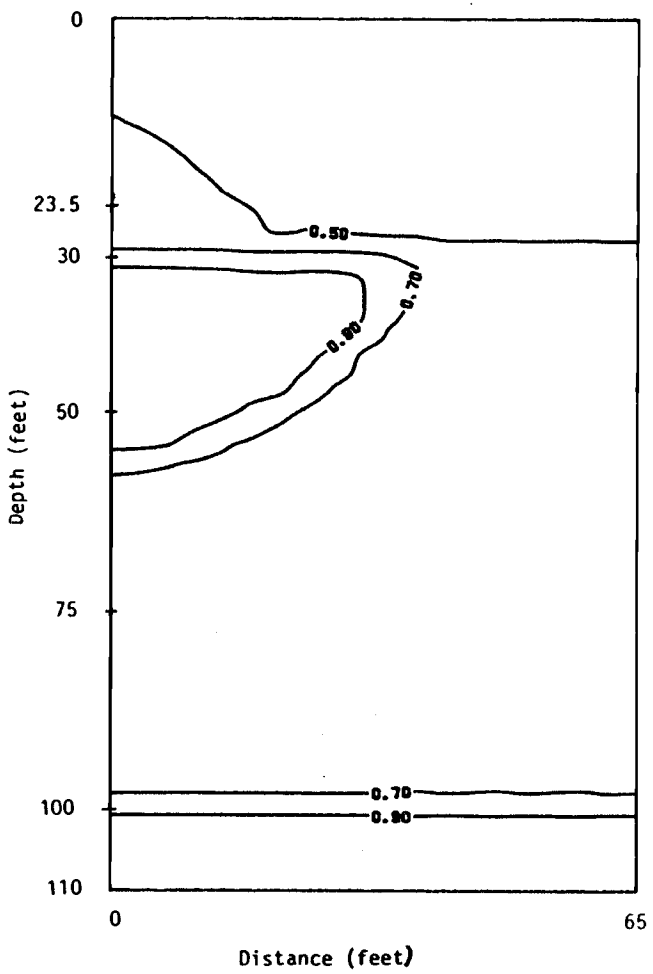

DEGREE OF SATURATION
5.50 HOURS OF POST-STORM 1 DRAINAGE
CASE 2: 8.327 HOURS TOTAL TIME

Fig. 21b

FIGURE 21

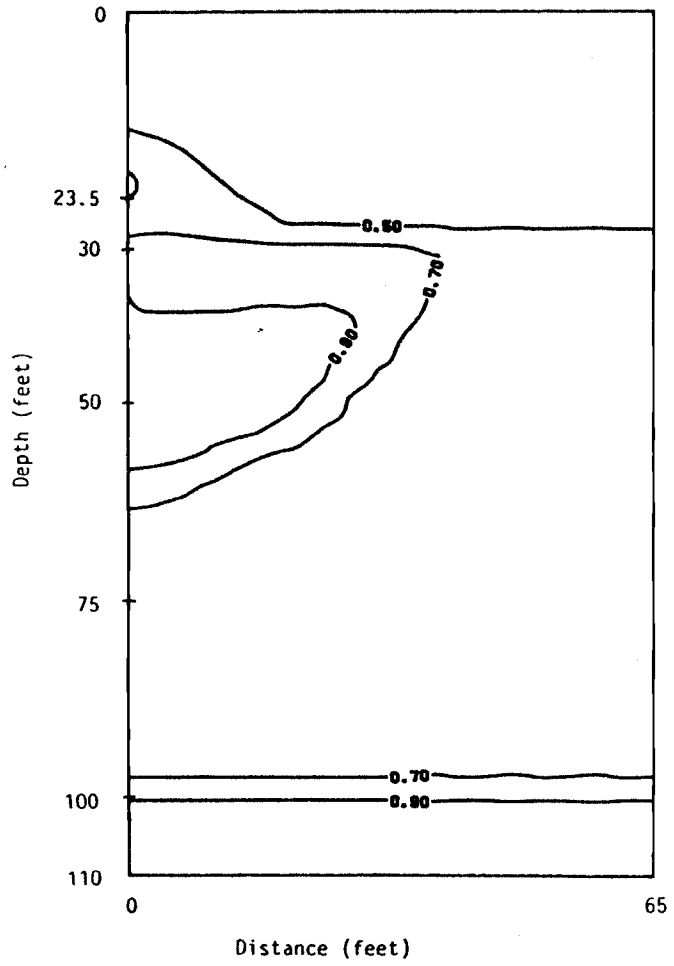

DEGREE OF SATURATION
24.00 HOURS OF POST-STORM 1 DRAINAGE
CASE 2: 26.827 HOURS TOTAL TIME

Fig. 22a

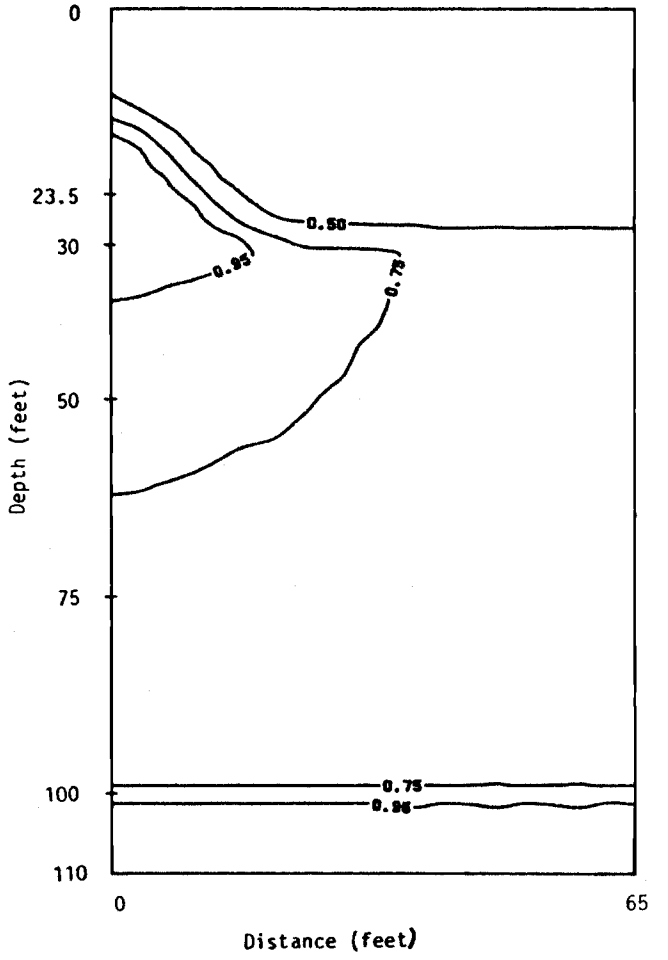

DEGREE OF SATURATION
0.50 HOURS OF INJECTION - STORM 2
CASE 2: 27.327 HOURS TOTAL TIME

Fig. 22b

FIGURE 22

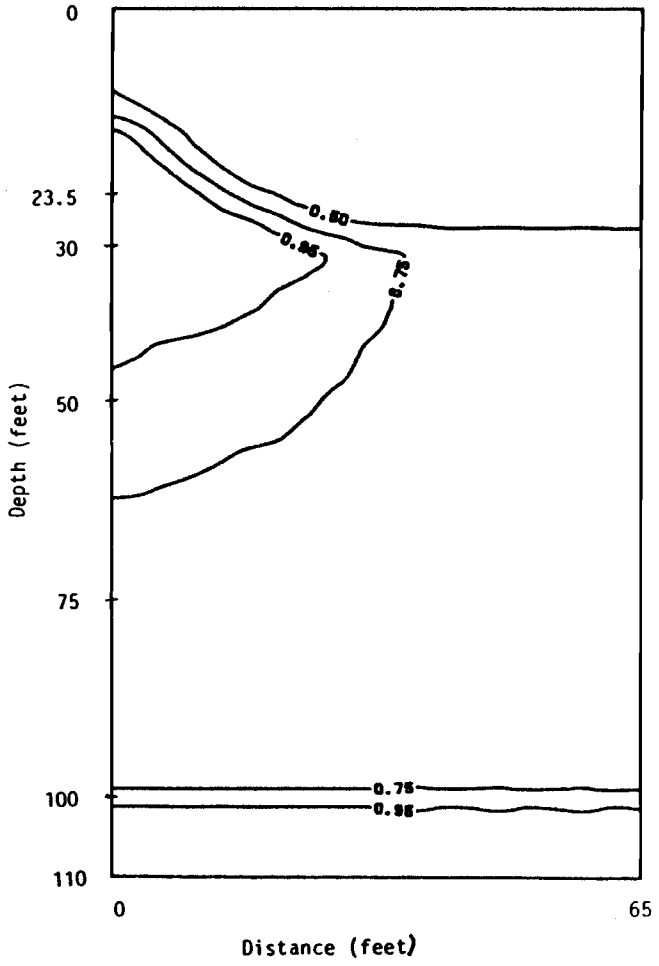

DEGREE OF SATURATION
1.25 HOURS OF INJECTION - STORM 2
CASE 2: 28.077 HOURS TOTAL TIME

Fig. 23a

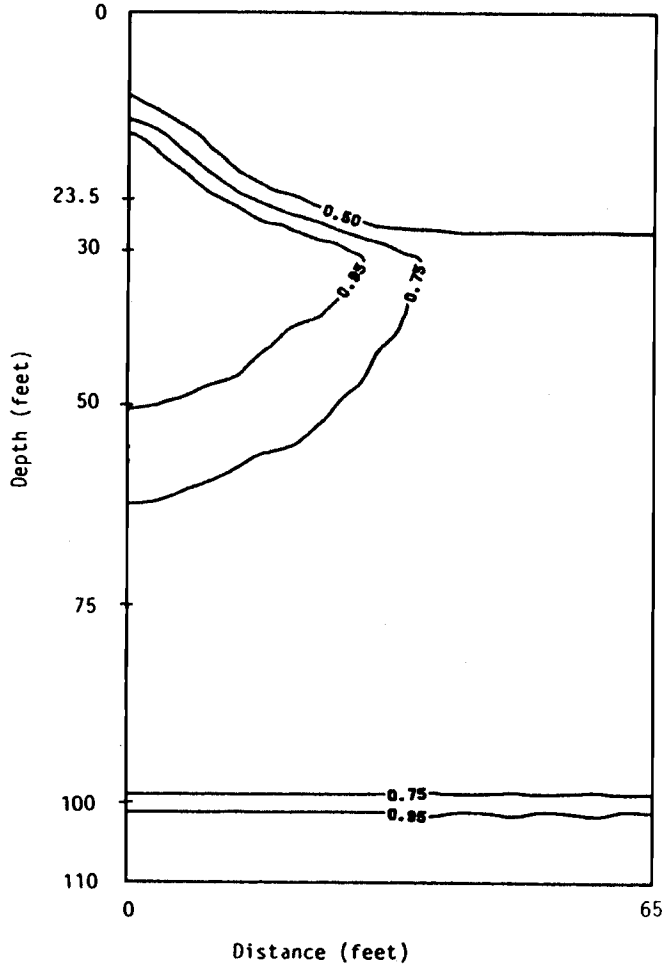

DEGREE OF SATURATION
1.75 HOURS OF INJECTION - STORM 2
CASE 2: 28.577 HOURS TOTAL TIME

Fig. 23b

FIGURE 23

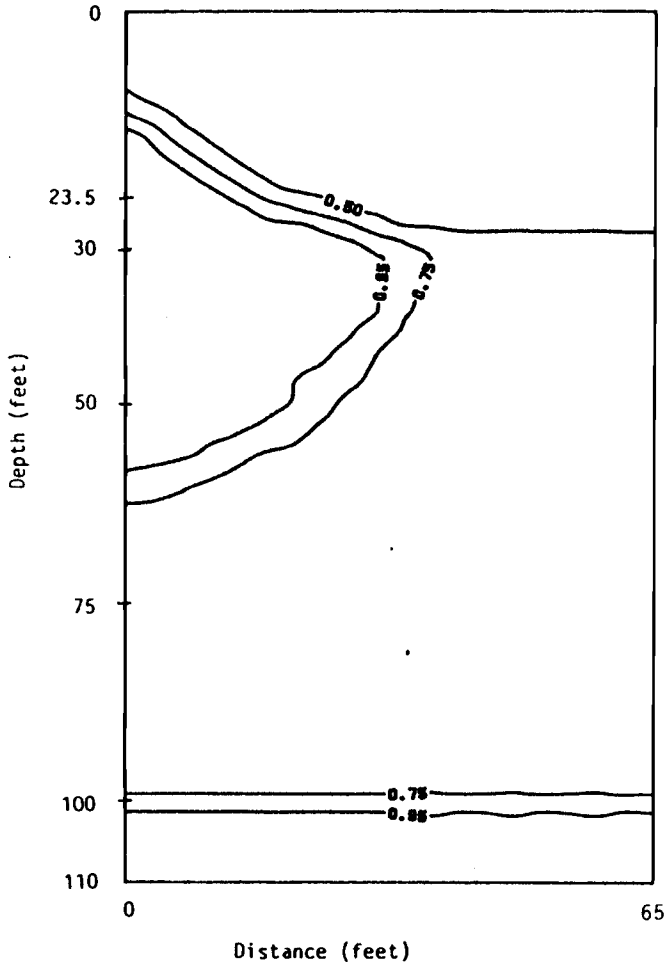

DEGREE OF SATURATION
2.629 HOURS OF INJECTION - STORM 2
CASE 2: 29.457 HOURS TOTAL TIME

Fig. 24a

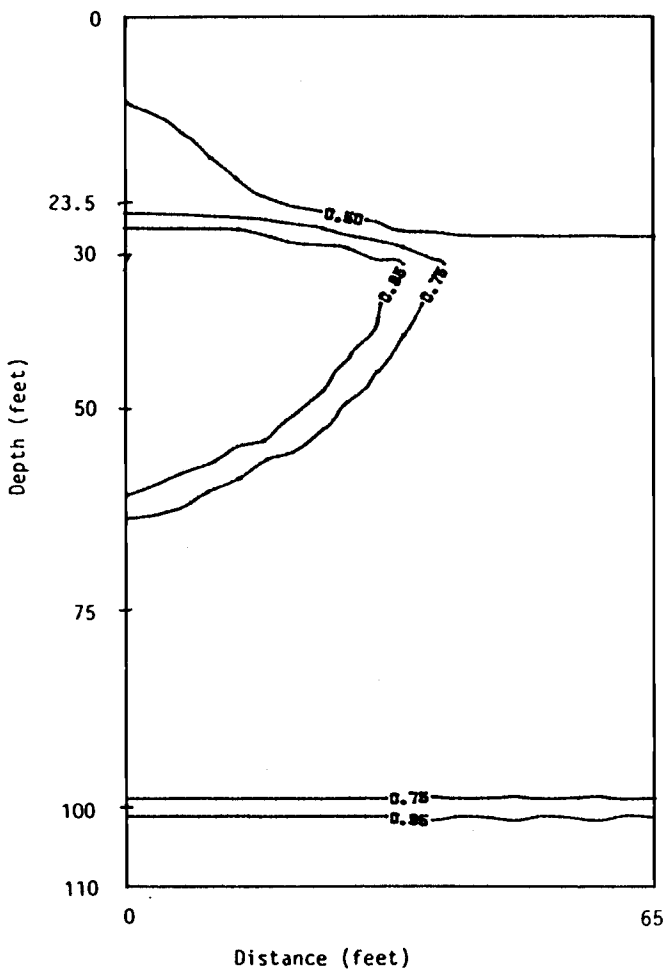

DEGREE OF SATURATION
0.50 HOURS OF POST-STORM 2 DRAINAGE
CASE 2: 29.957 HOURS TOTAL TIME

Fig. 24b

FIGURE 24

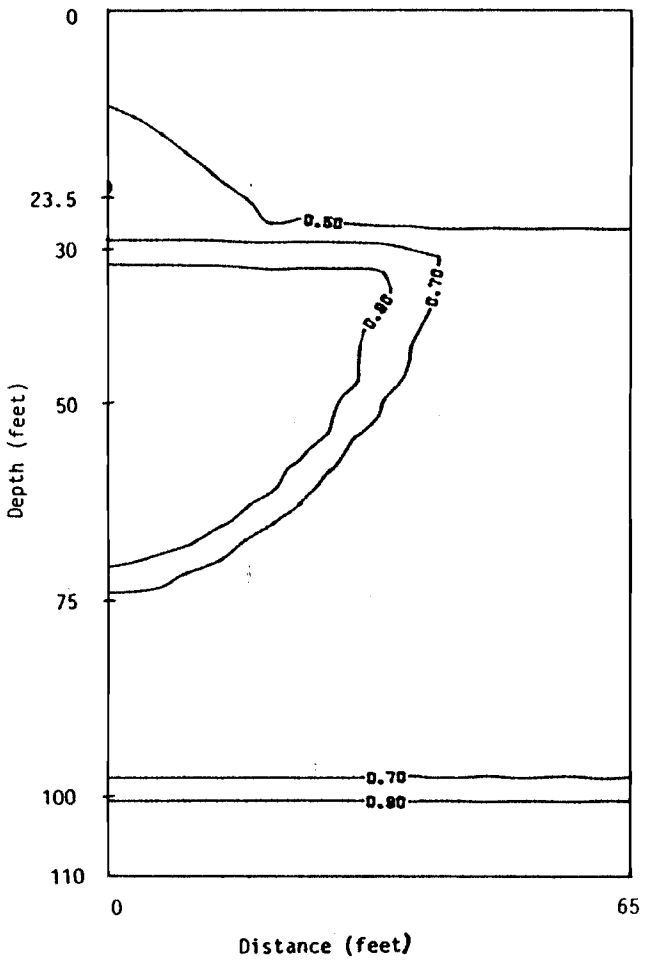

DEGREE OF SATURATION
9.00 HOURS OF POST-STORM 2 DRAINAGE
CASE 2: 38.457 HOURS TOTAL TIME

Fig. 25a

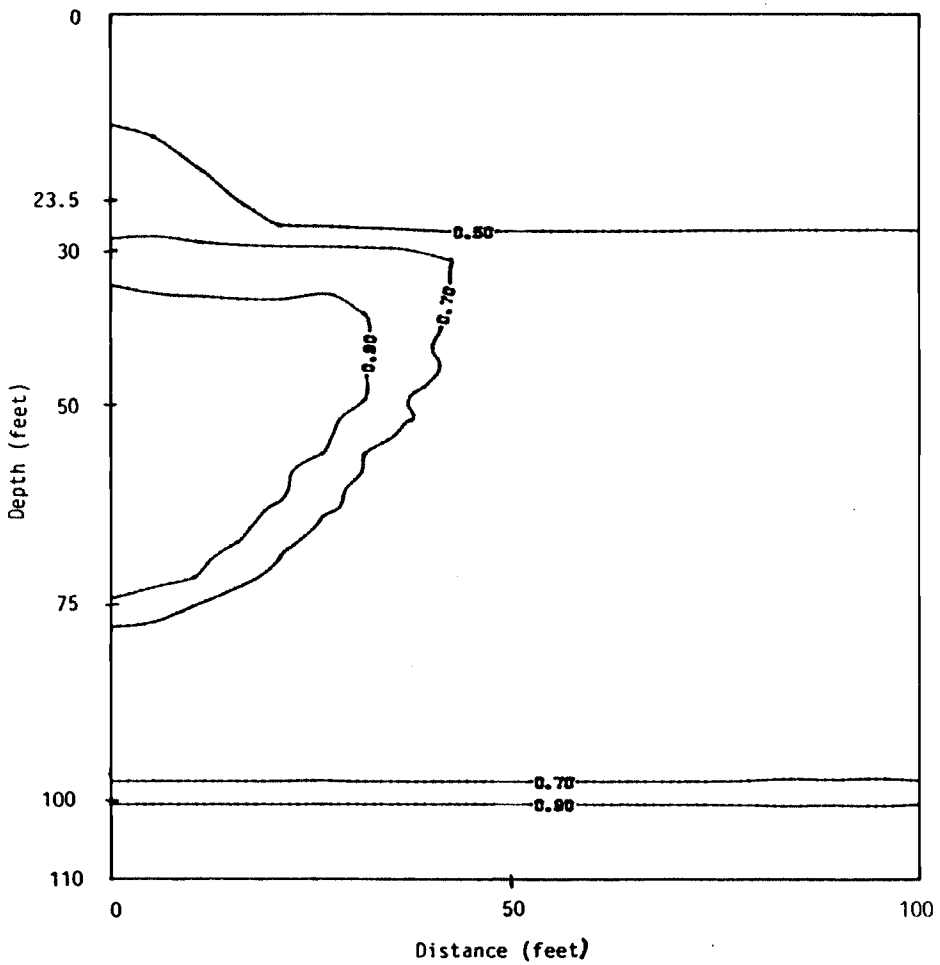

DEGREE OF SATURATION
20.00 HOURS OF POST-STORM 2 DRAINAGE
CASE 2: 49.457 HOURS TOTAL TIME

Fig. 25b

FIGURE 25

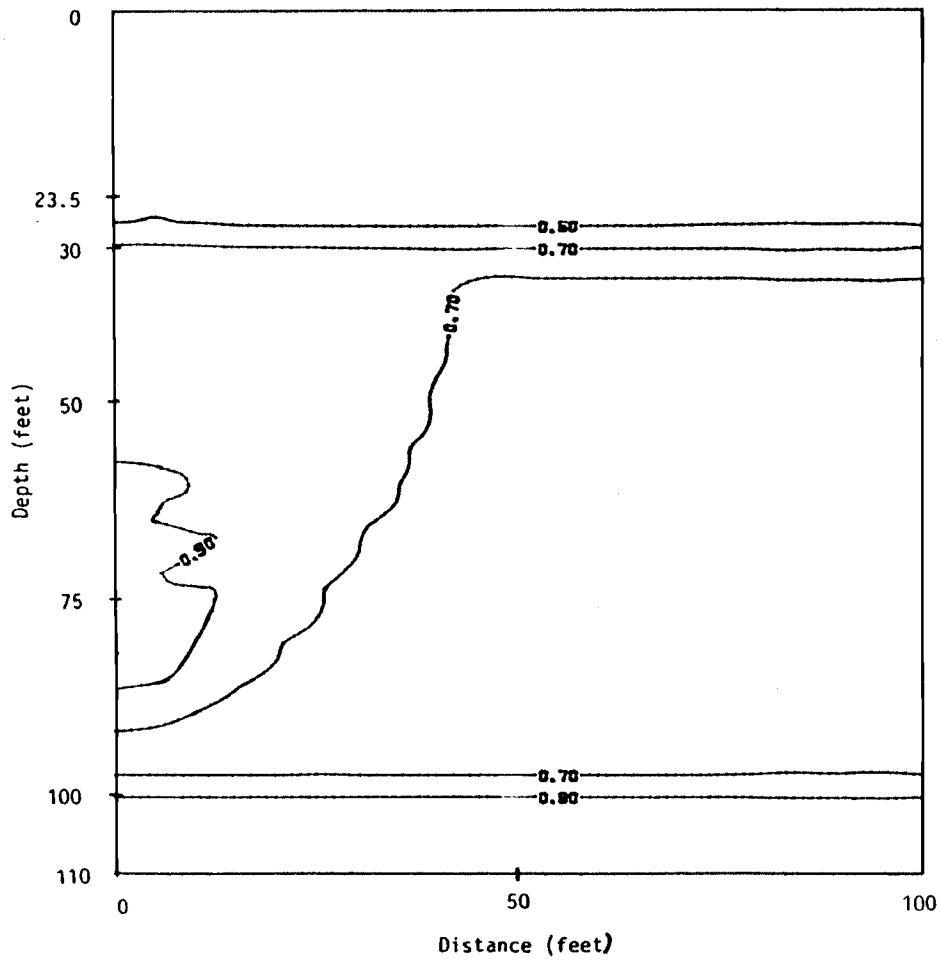

DEGREE OF SATURATION
130.00 HOURS OF POST-STORM 2 DRAINAGE
CASE 2: 159.457 HOURS TOTAL TIME

Fig. 26a

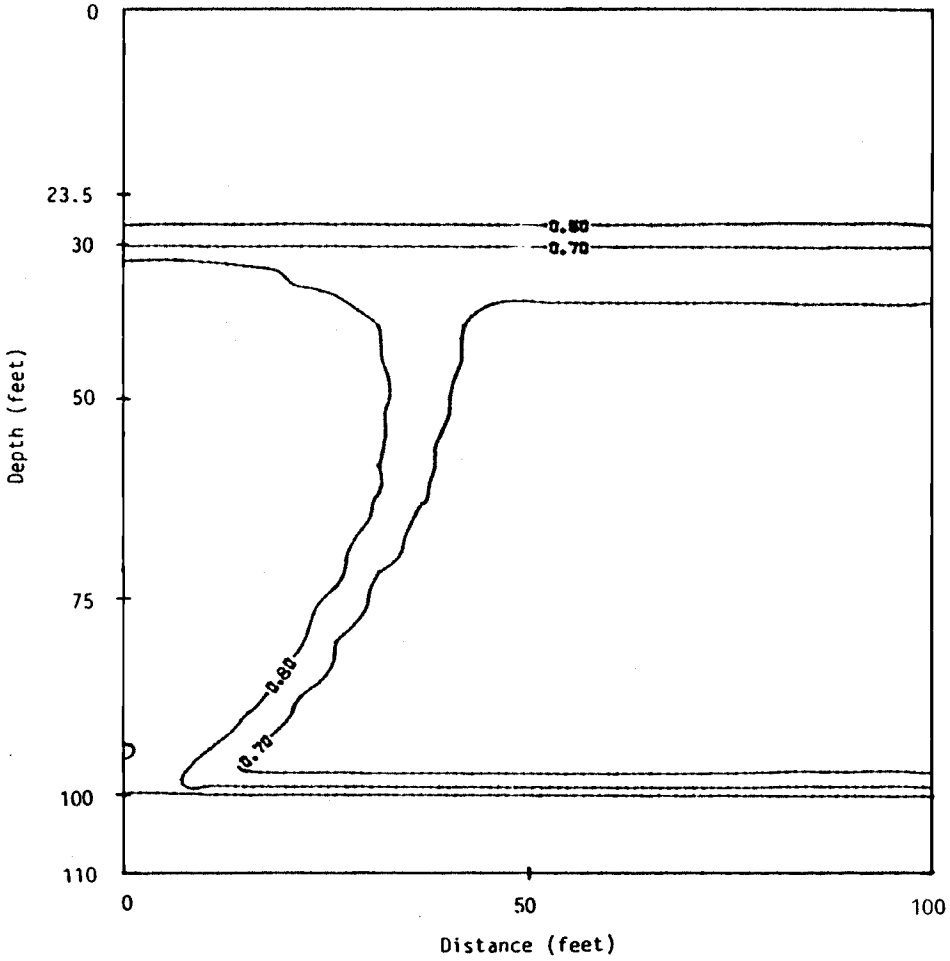

DEGREE OF SATURATION
262.00 HOURS OF POST-STORM 2 DRAINAGE
CASE 2: 291.457 HOURS TOTAL TIME

Fig. 26b

FIGURE 26

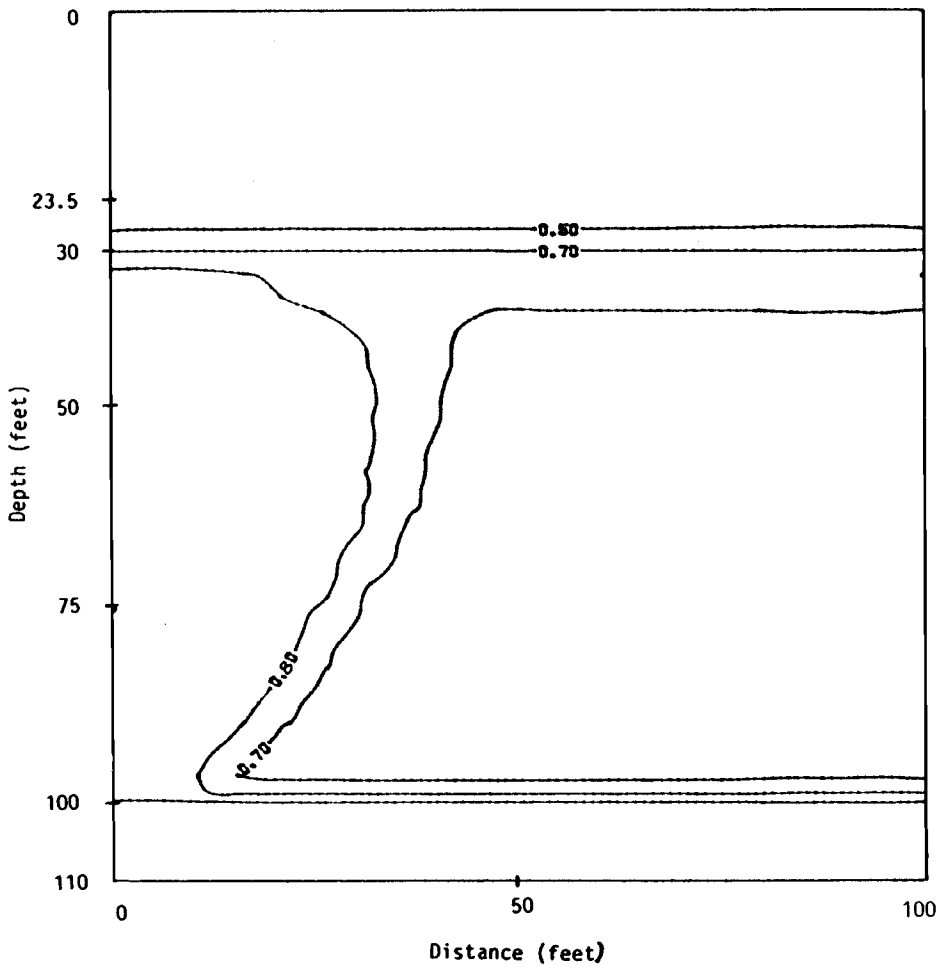

DEGREE OF SATURATION
286.00 HOURS OF POST-STORM 2 DRAINAGE
CASE 2: 315.457 HOURS TOTAL TIME

FIGURE 27

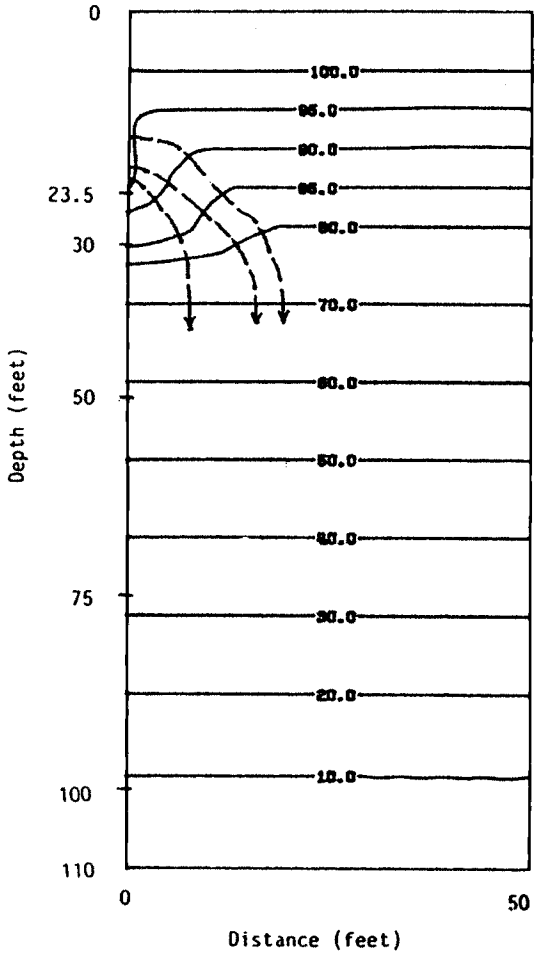

HYDRAULIC HEAD DISTRIBUTION (FEET)
0.50 HOURS OF INJECTION
CASE 2; STORM 1

Fig. 28a

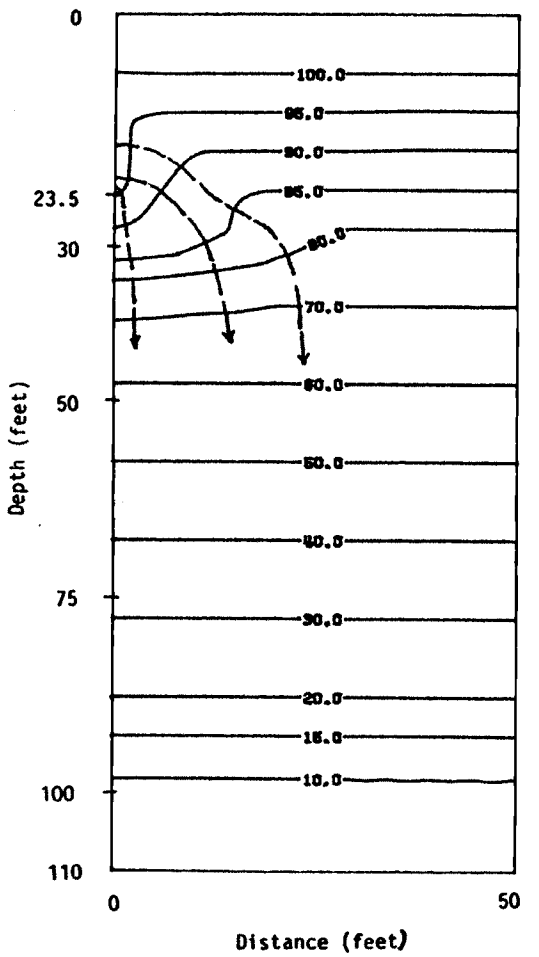

HYDRAULIC HEAD DISTRIBUTION (FEET)
1.66 HOURS OF INJECTION
CASE 2; STORM 1

Fig. 28b

FIGURE 28

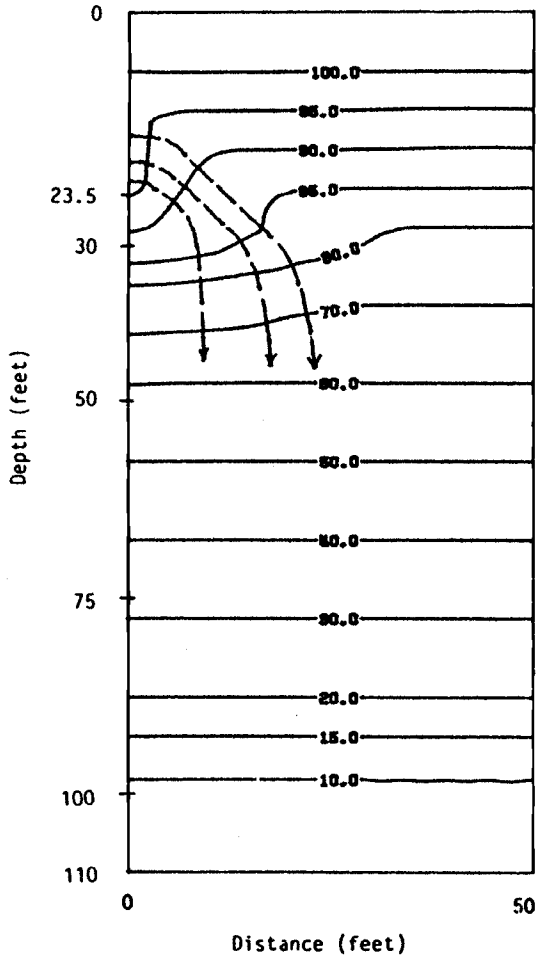

HYDRAULIC HEAD DISTRIBUTION (FEET)
2.827 HOURS OF INJECTION - 5000 CU. FT.
CASE 2; STORM 1

Fig. 29a

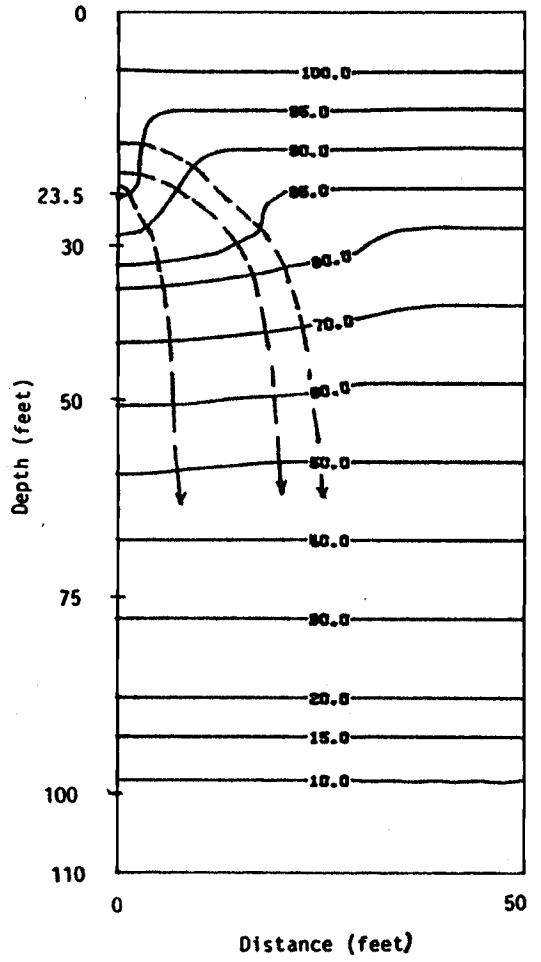

HYDRAULIC HEAD DISTRIBUTION (FEET)
2.629 HOURS OF INJECTION; STORM 2
29.457 HOURS TOTAL TIME

Fig. 29b

FIGURE 29

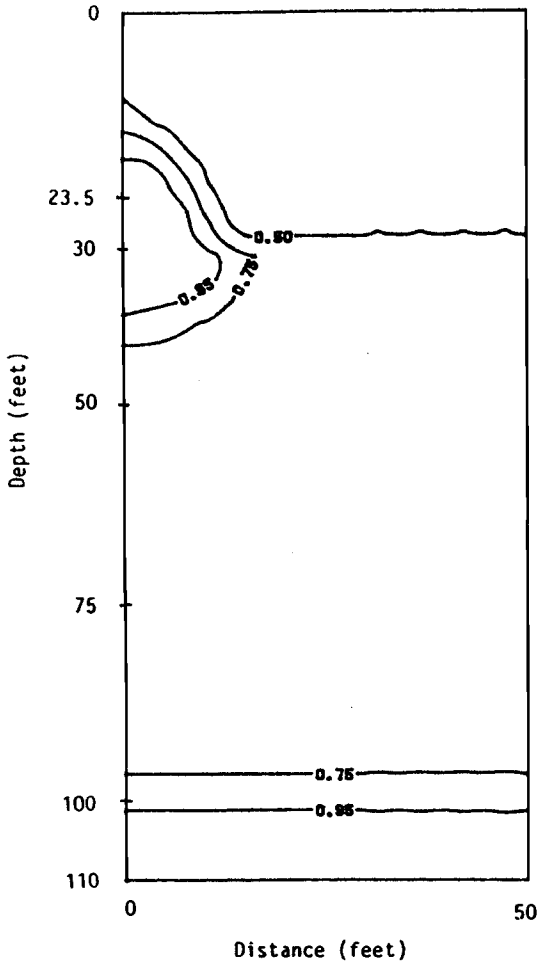

DEGREE OF SATURATION
0.50 HOURS OF INJECTION
CASE 3; STORM 1

Fig. 30a

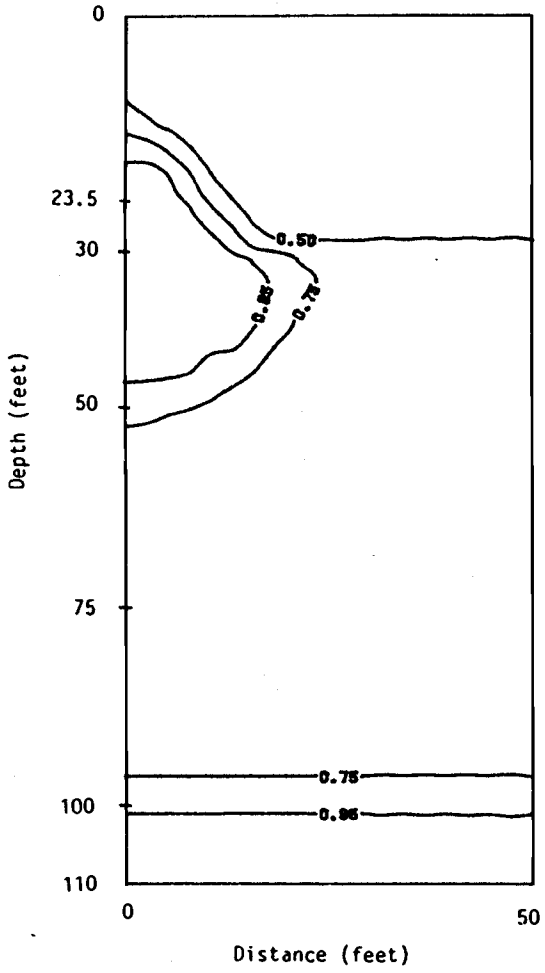

DEGREE OF SATURATION
1.166 HOURS OF INJECTION
CASE 3; STORM 1

Fig. 30b

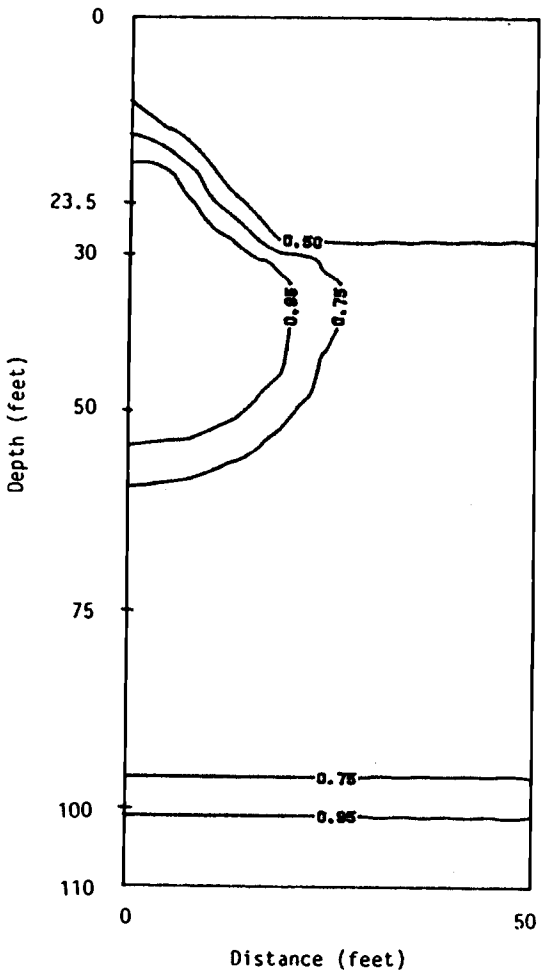

DEGREE OF SATURATION
2.00 HOURS OF INJECTION
CASE 3; STORM 1

Fig. 30c

FIGURE 30

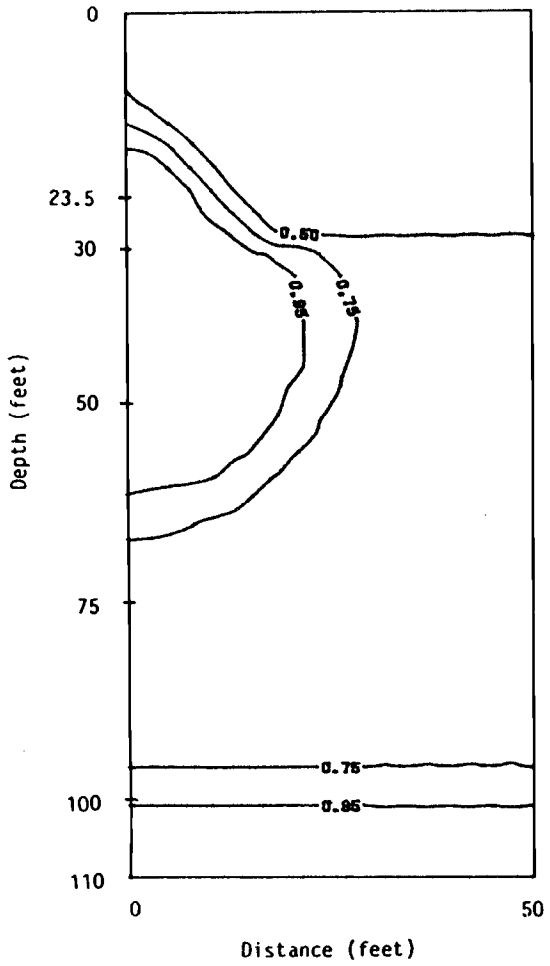

DEGREE OF SATURATION
2.75 HOURS OF INJECTION -
5000 CU. FT.
CASE 3: STORM 1

Fig. 31a

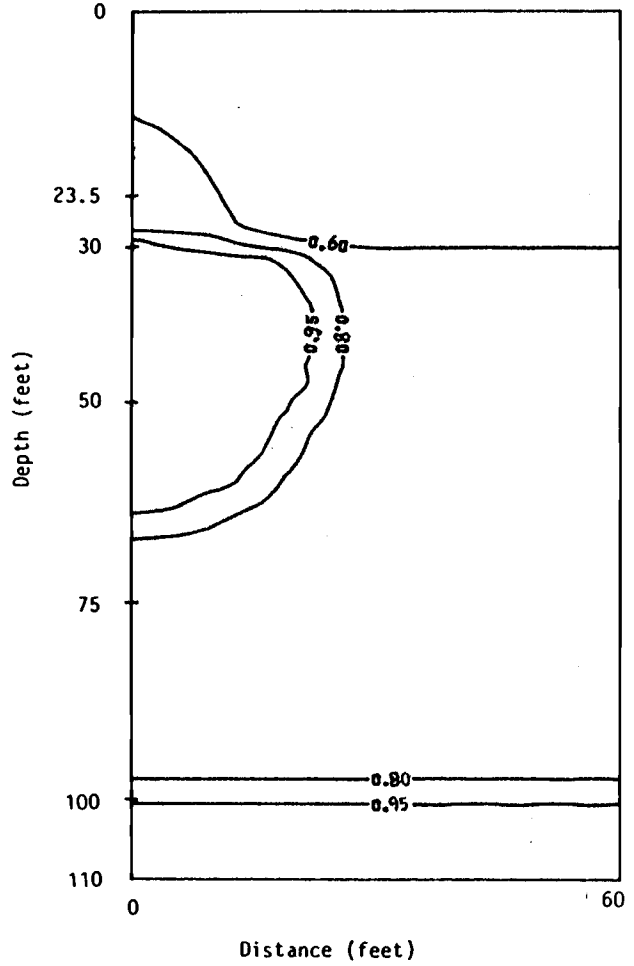

DEGREE OF SATURATION
0.50 HOURS OF POST-STORM 1 DRAINAGE
CASE 3: 3.25 HOURS TOTAL TIME

Fig. 31b

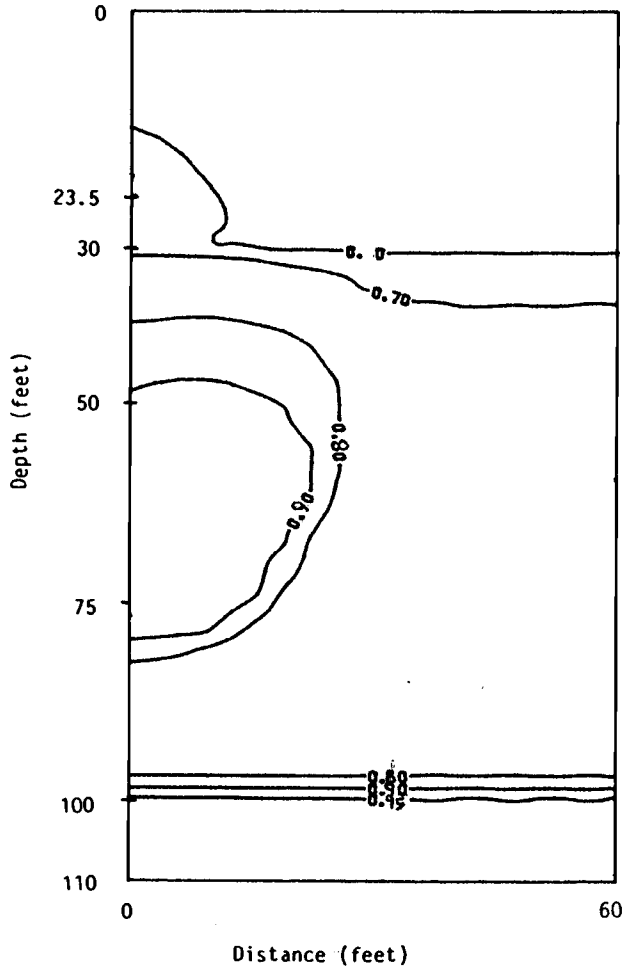

DEGREE OF SATURATION
2.75 HOURS OF POST-STORM 1 DRAINAGE
CASE 3: 5.50 HOURS TOTAL TIME

Fig. 31c

FIGURE 31

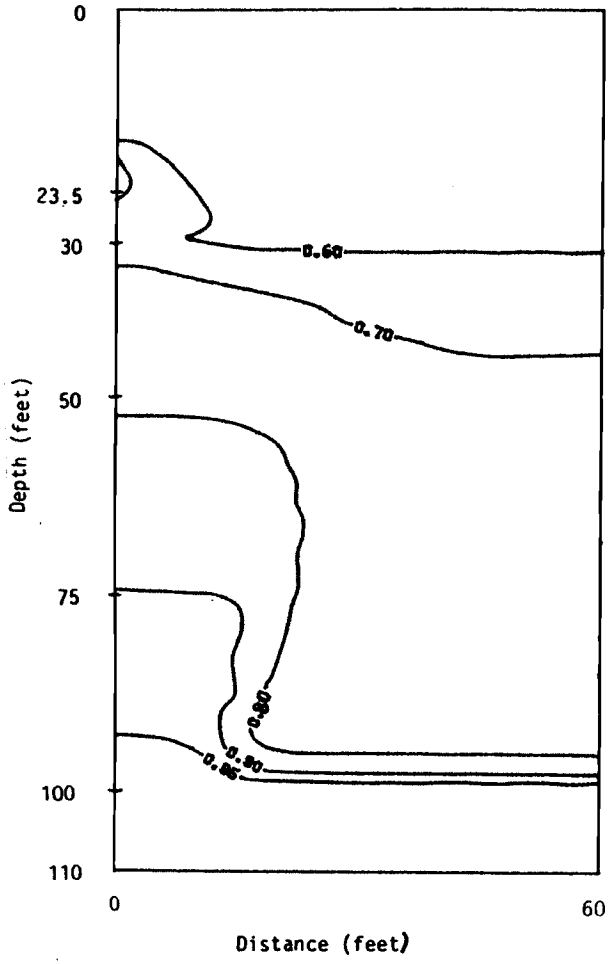

DEGREE OF SATURATION
6.25 HOURS OF POST-STORM 1 DRAINAGE
CASE 3: 9.00 HOURS TOTAL TIME

Fig. 32a

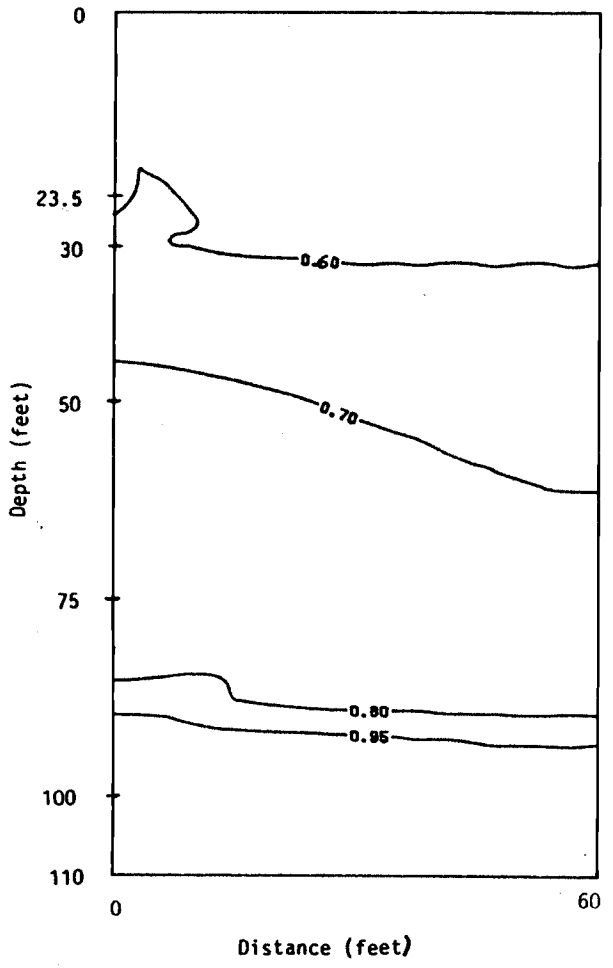

DEGREE OF SATURATION
14.25 HOURS OF POST-STORM 1 DRAINAGE
CASE 3: 17.00 HOURS TOTAL TIME

Fig. 32b

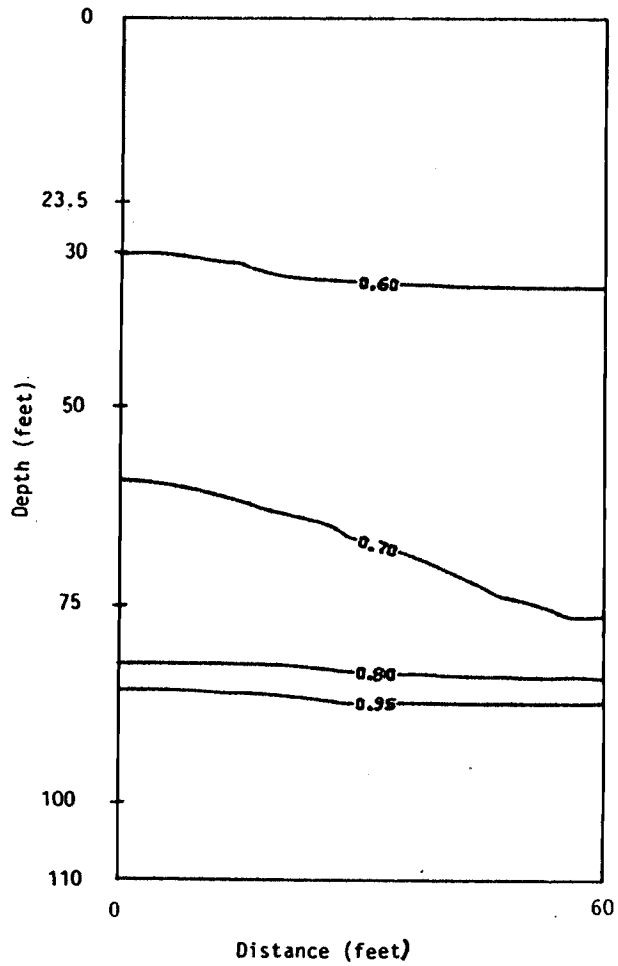

DEGREE OF SATURATION
24.00 HOURS OF POST-STORM 1 DRAINAGE
CASE 3: 26.75 HOURS TOTAL TIME

Fig. 32c

FIGURE 32

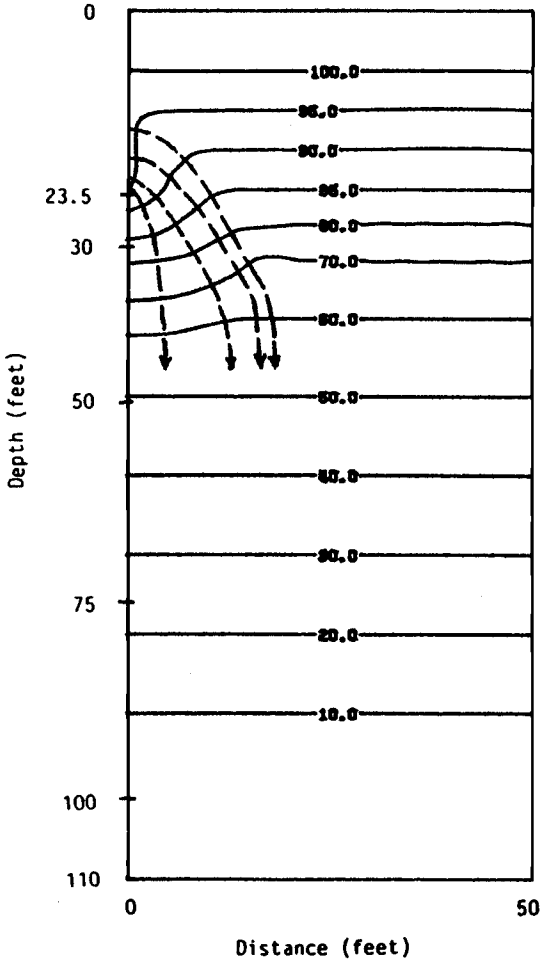

HYDRAULIC HEAD DISTRIBUTION (FEET)
2.75 HOURS OF INJECTION - 5000 CU. FT.
CASE 3; STORM 1

Fig. 33a

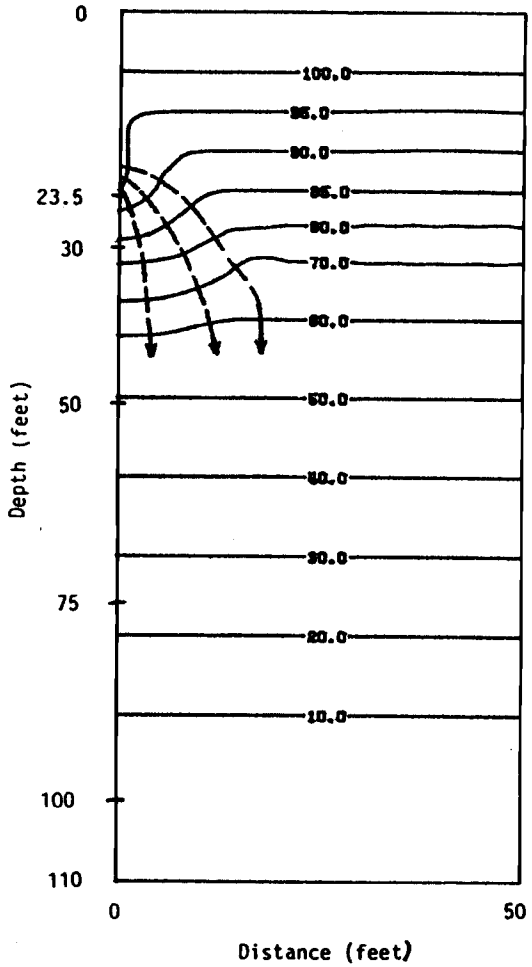

HYDRAULIC HEAD DISTRIBUTION (FEET)
0.500 HOURS OF INJECTION
CASE 3; STORM 1

Fig. 33b

FIGURE 33